



Experimental studies of aqueous alteration of chondrules in the carbonaceous chondrites

大西, 市朗

(Degree)

博士 (理学)

(Date of Degree)

2003-03-31

(Date of Publication)

2007-08-27

(Resource Type)

doctoral thesis

(Report Number)

甲2787

(URL)

<https://hdl.handle.net/20.500.14094/D1002787>

※ 当コンテンツは神戸大学の学術成果です。無断複製・不正使用等を禁じます。著作権法で認められている範囲内で、適切にご利用ください。



博士論文

炭素質コンドライト中の
コンドルール水質変成に関する実験的研究

平成 15 年 1 月

神戸大学大学院自然科学研究科

大西 市朗

Doctoral Dissertation

Experimental studies of aqueous alteration of chondrules in the carbonaceous chondrites

January, 2003

Graduate School of Science and Technology, Kobe University

Ichiro Ohnishi

Contents

<i>Preface</i>	6
Part I	
Hydrothermal experiments of enstatite: An attempt to simulate aqueous alteration of chondrules in the carbonaceous chondrites	8
Chapter 1 General Introduction	9
1.1 Previous low-temperature hydrothermal experiments to clarify aqueous alteration of the carbonaceous chondrites	9
1.2 Characteristics of aqueously altered enstatite in the carbonaceous chondrites	10
1.2.1 Alteration products	10
1.2.2 Alteration textures	11
1.3 The purposes of hydrothermal experiments of enstatite	13
Chapter 2 Experimental Procedures	14
2.1 Starting Materials	14
2.2 Hydrothermal Experiments	17
2.3 Characterization of Products	21
Chapter 3 Results:	
Hydrothermal products and textural characteristics of altered enstatite	22
3.1 Results of Experiment 1	22
3.1.1 pH and composition of aqueous solution	22
3.1.2 Experimental temperature	24
3.1.3 Duration time	26
3.1.4 Summary	28
3.2 Results of Experiment 2	29

3.3 Results of Experiment 3	30
3.3.1 SEM analysis	30
3.3.2 TEM analysis	32
Chapter 4 Discussion:	
Alteration mechanism of enstatite and aqueous alteration process of chondrites	34
4.1 Products of Experiments	34
4.1.1 Formation process of smectite from enstatite	34
4.1.2 Formation process of serpentine from enstatite	36
4.1.3 Acidic conditions	38
4.2 Comparison of hydrothermal experimental products with secondary minerals in aqueous altered chondrites	39
4.2.1 Comparison with enstatite in chondrules of CV chondrites	39
4.2.2 Comparison with enstatite in chondrules of CM chondrites	40
4.3 Aqueous alteration scenarios of chondrites	42
4.3.1 Aqueous alteration scenario of CV chondrites	42
4.3.2 Aqueous alteration scenario of CM chondrites	43
4.3.3 Initial water/rock ratio and pH of aqueous solution	46
4.4 Comparison of textures of hydrothermal altered enstatite with those of naturally altered enstatite in chondrites	47
4.4.1 Crystallographic features of enstatite alteration	47
4.4.2 Crystallographic relationships between enstatite and the secondary minerals	49
Conclusions for Part I	51
References for Part I	53
Part II	
Modeling aqueous alteration of chondrules: Result of the Geochemist's workbench	58
Chapter 5 General Introduction	59
5.1 Previous modeling studies of aqueous alteration of the carbonaceous chondrites using computer code	59

5.2 Aqueous alteration of chondrules	59
5.3 The purposes of modeling of aqueous alteration of chondrules	60
Chapter 6 Computer Simulations	61
6.1 Scenarios of aqueous alteration of chondrules	61
6.1.1 Model 1	61
6.1.2 Model 2	62
6.1.3 Model 3	62
6.2 Modeling study	64
Chapter 7 Results and Discussion	66
7.1 Comparison of the predicted mineral assemblage from GWB with alteration mineral assemblage in chondrules	67
7.1.1 Model 1	67
7.1.2 Model 2	68
7.1.3 Model 3	68
Conclusions for Part II	74
References for Part II	75
Chapter 8 Concluding Remarks of This Thesis	78
Acknowledgement	79

Preface

Extensive development of hydrous secondary minerals observed in many classes of chondritic meteorites indicates that aqueous alteration was one of the most widespread of the alteration processes, which have affected the primary materials formed in the solar nebula. Aqueous alteration is widely considered to have occurred in the chondritic parent bodies (*i.e.*, comets or asteroidal parent bodies). Thus, clarification of condition and mechanism of aqueous alteration is important to understand the evolutionary history of the parent bodies.

Chondrules are the most abundant components of chondritic meteorites. They comprise <80% of ordinary and enstatite chondrites and >15% of carbonaceous chondrites except for CI clan, which lacks chondrules. They are sub-millimeter-sized igneous spherules composed mainly of ferromagnesian silicates (olivine, pyroxene, and a feldspathic glass). The primary mineralogy of chondrules has been modified by aqueous alteration in various degrees, and the aqueously altered chondrules contain secondary hydrous phyllosilicates, hydroxides, carbonates and sulfates. The aqueous alteration process of chondrules is considered to reflect that of bulk chondrites, and so, to unravel the alteration process of chondrules is important for understanding condition and mechanism of aqueous alteration of chondrites.

Enstatite is one of the most common minerals in chondrules. Systematic petrologic studies reveal that enstatite has been more strongly altered to hydrous phyllosilicates than any other silicates in chondrules (*e.g.*, Hanowski and Brearley, 2001). Thus, enstatite could be regarded as an indicator of aqueous alteration of chondrules. However, the alteration mechanism of enstatite has been poorly understood. In order to examine secondary mineral assemblage formed by aqueous alteration of enstatite under various conditions, I carried out the hydrothermal experiments of enstatite powders with or without Fe powders for a wide range of temperature (100-300°C), pH (0-14) of aqueous solution, and duration time (24-336 hours). And I also performed the experiments using enstatite single crystals of different polymorph (orthoenstatite or clinoenstatite) to examine alteration texture of enstatite. In part I, I discussed the alteration mechanism of enstatite and tried to clarify the alteration process

of chondrules.

In order to understand physic-chemical conditions of aqueous alteration, many workers have performed modeling studies using computer code (*e.g.*, Zolensky et al., 1989). In part II, I modeled the aqueous alteration process of chondrules and predicted the alteration mineral assemblages, using the REACT computer code (Bethke, 1996) that is one of the major geochemical modeling tools. Then, I compared the predicted alteration mineral assemblage with natural alteration mineral assemblage to discuss the alteration process of chondrules.

Although the petrology and mineralogy of the aqueous alteration in chondrites became increasingly well understood, we have not yet obtained the details about aqueous alteration. In an effort to obtain part of the question, we should take another approach, that is, the experimental studies. The main purpose of this thesis is to investigate the quantitative parameters controlling the aqueous alteration process of chondrules by experimental approaches (hydrothermal experiment or computer modeling), in order to unravel aqueous alteration of chondrites.

Part I

**Hydrothermal experiments of enstatite:
An attempt to simulate aqueous alteration
of chondrules in the carbonaceous chondrites**

Chapter 1

General Introduction

1.1 Previous low-temperature hydrothermal experiments to clarify aqueous alteration of the carbonaceous chondrites

As well as abundant secondary hydrous phases observed in the CI and CM carbonaceous chondrites, meteorites in numerous other chondrite clans, such as the CR, CV, CO carbonaceous chondrites and unequilibrated ordinary chondrites also contained a various amount of hydrous phases. Thus, aqueous alteration was one of the most widespread of the alteration processes, which have affected chondritic meteorites. Although the mineralogy of secondary hydrous phases such as phyllosilicates, hydroxide, carbonate and sulfate observed in chondrites has become increasingly well understood, we have not yet obtained the important information about aqueous alteration. These include location where the alteration has occurred (*i.e.*, nebular or parent body) and timing when the alteration has occurred. In an effort to obtain the information, we must understand such fundamental knowledge as the conditions, time scales and the mechanisms of alteration process. Experimental studies can partially address some of these questions by examining the kinetics of aqueous alteration reactions.

Many workers have conducted low-temperature hydrothermal experiments (50-450°C) in the past decade (Table 1.1). Most of them have used solid chips of chondritic meteorite, including Allende (CV), Murchison (CM) and Nuevo Mercurio (H5), as starting materials (Tomeoka and Kojima, 1995; Kojima and Tomeoka, 1999, 2000; Brearley and Duke, 1998; Duke and Brearley, 1998, 1999; Jones and Brearley, 2000; Brearley and Jones, 2002; Sato et al., 2002). These experiments have assessed spatial relationship between reactant and product phases, and bulk changes of chemical composition, pH and ion concentration of aqueous solution. On the other hands, some workers have used chondritic component minerals, including olivine solid solution

(Takatori et al., 1993; Iishi et al., 1997; Iishi and Han, 1999), refractory minerals (Nomura and Miyamoto, 1998), as starting materials. These experiments have explored elemental reaction processes of alteration, kinetic of reaction, and growth mechanism of new phase to reveal local changes in aqueous alteration. The carbonaceous chondrites consist of a variety of components that distribute in the order of sub-mm scales and aqueous alteration would not reach the equilibrium. Thus, the experiments using chondritic component minerals as starting materials are more useful to unravel the mechanisms of aqueous alteration processes in the carbonaceous chondrites compared with those using bulk meteorites.

Table 1.1: Lists of previous low-temperature (50-450°C) hydrothermal experiments.

	Literature	Starting materials	Solutions	Temperature(°C)	Pressure(bars)	Duration time	Atmospheric conditions	Water/rock ratio
Bulk samples	Tomeoka and Kojima (1995)	Allende(CV3)	1N-HCl	450	800	4-6 weeks	oxidizing	1.7 ^c
	Kojima and Tomeoka (1999, 2000)	Allende(CV3)	1N-HCl, H ₂ O	450	800	7 weeks	oxidizing	1.7 ^c
	Brearley and Duke (1998)	Allende(CV3)	H ₂ O	150-200	Auto. ^b	1 week-2 months	oxidizing	1.0-6.0 ^d
	Duke and Brearley (1999)	Allende(CV3)	H ₂ O	200	Auto. ^b	30-90 days	reducing	1.0-6.0 ^d
	Jones and Brearley (2000)	Allende(CV3)	H ₂ O	100-200	Auto. ^b	7-180 days	oxidizing, reducing	1.0-8.0 ^d
	Brearley and Jones (2002)	Allende(CV3)	H ₂ O	100-200	Auto. ^b	1 week-6 months	oxidizing	1.0-9.0 ^d
	Sato et al. (2002)	Allende(CV3), Muchison(CM2), Nuevo Mercurio(H5)	H ₂ O	50-200	Auto. ^b	2-168 hours	oxidizing, reducing	3333- 5000 ^c
Minerals	Takatori et al. (1993)	Ol s.s. ^a (Fa ₀₋₁₀₀)	1N-HCl, H ₂ O	400	500	1 week	oxidizing	4 ^c
	Iishi et al. (1997)	Ol s.s. ^a (Fa ₇₀₋₁₀₀)	1N-NaOH	300	100	1 week-1 month	oxidizing	0.6-1.7 ^c
	Iishi and Han (1999)	Ol s.s. ^a (Fa ₅₀₋₁₀₀)	1N-NaOH, Albite-comp., En-comp., Matrix-comp.	50-200	Auto. ^b	2 week-2 month	oxidizing	40 ^c
	Nomura and Miyamoto (1998)	Refractory minerals	0.01-1N HCl, 1-2N Na ₂ CO ₃ , 0.01-5N NaOH, H ₂ O, 2N-Na ₂ SO ₄	200-250, 400	Auto. ^b , 500	48-168, 168 hours	oxidizing	4.7-47 ^c

^as.s.=solid solution.

^bAuto.=Autogeneous water vapor pressure.

^cweight ratio.

^dvolume ratio.

1.2 Characteristics of aqueously altered enstatite in the carbonaceous chondrites

1.2.1 Alteration products

Enstatite is one of the most common minerals and occurs widely as phenocrysts of chondrules in the carbonaceous chondrites. In CM and CV chondrite clans, enstatite phenocrysts have been widely altered to hydrous phyllosilicates. The phyllosilicate produced in CM chondrites has been mostly ferroan Mg-rich serpentine (Fig. 1.1)

(Hanowski and Brearley, 2001). On the other hands, the phyllosilicate produced in CV chondrites has been mostly smectite such as saponite (Fig. 1.1) (Keller and Buseck, 1990). The difference of phyllosilicate mineralogy between these chondrite clans regardless of the same precursor mineral (*i.e.*, enstatite) probably indicates that aqueous alteration condition has differed between these chondrite clans: reaction temperature, pH of aqueous solution, gas fugacity, duration time, etc.

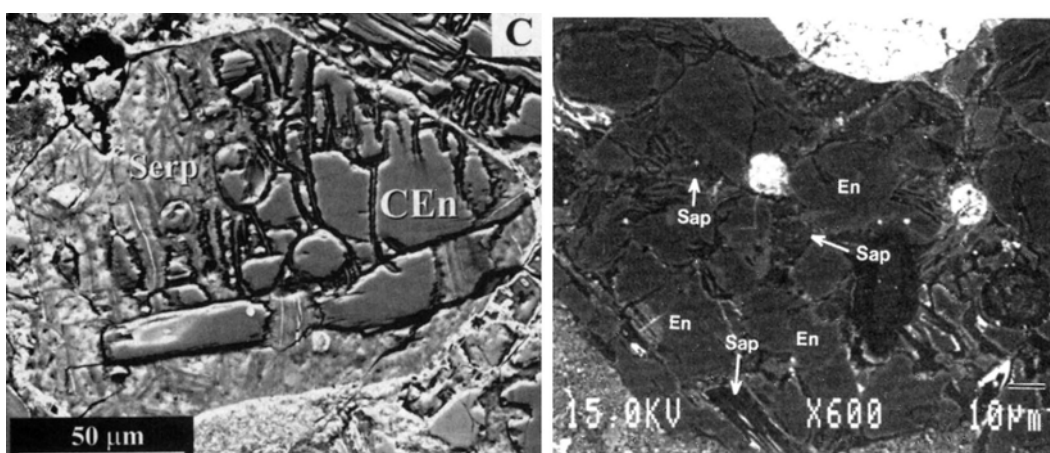


Figure 1.1: Backscattered electron images of altered enstatite in chondrules of Allan Hills 81002 CM carbonaceous chondrite (left; Hanowski and Brearley, 2001) and Kaba CV carbonaceous chondrite (right; Keller and Buseck, 1990). In CM chondrite, clinoenstatite (CEn) phenocryst is altered to serpentine (Serp), while, in CV chondrite, enstatite (En) phenocrysts are altered to saponite (Sap).

1.2.2 Alteration textures

Enstatite of chondrule phenocryst has two polymorphs: clinoenstatite (space group $P2_1/c$) and orthoenstatite ($Pbca$). In petrologic type lower than 3, chondrules contain abundantly clinoenstatite and less or no orthoenstatite. Clinoenstatite would be formed by the inversion from protoenstatite that has firstly crystallized during chondrule solidification by quenching of melt droplet (*e.g.*, Brearley and Jones, 1998). Numerous systematic analyses of the textural and compositional relationship between unaltered and altered enstatite in chondrules of aqueous altered chondrites (*e.g.*, Hanowski and Brearley, 2001) have provided evidence that clinoenstatite tends to have less resistance to the alteration compared with orthoenstatite and any other silicates in chondrules (Fig. 1.2).

Transmission electron microscope (TEM) analyses of chondrules in aqueously altered CV chondrites have recognized that there is the crystal orientation relationship

between altered enstatite and the secondary mineral (*e.g.*, Keller and Buseck, 1990) (Fig. 1.2). On the other hands, TEM analyses of chondrules in CM chondrites have not recognized the crystal relationship (*e.g.*, Hanowski and Brearley, 1997). They suggest that the alteration of enstatite would show crystallographic variations between these chondrite clans.

These textural alteration features suggest that the differences in resistance of enstatite to alteration between minerals or each mineral depend strongly on the crystal structure. We should obtain the knowledge about textural characteristics of altered enstatite and relationship between altered enstatite and the secondary mineral in details.

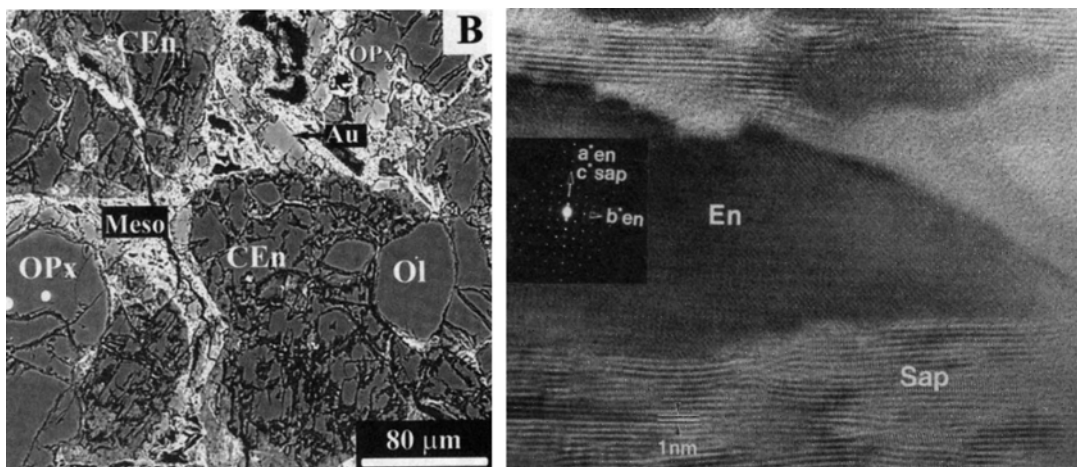


Figure 1.2: (Left image) Backscattered electron image of the portion of chondrule in Allan Hills 81002 CM carbonaceous chondrite (Hanowski and Brearley, 2001). Clinoenstatite (CEn) phenocrysts and mesostasis (Meso) have been extensively replaced by secondary minerals, while orthoenstatite (Opx), augite (Au) and olivine (Ol) phenocrysts not so. (Right image) High-resolution transmission electron image of an oriented intergrowth of saponite (Sap) and enstatite (En) in Kaba CV carbonaceous chondrite. The selected area electron diffraction pattern shows that a^* of enstatite parallels c^* of saponite.

1.3 The purposes of hydrothermal experiments of enstatite

Enstatite in chondrules of aqueously altered chondrites has showed a variety of characteristics in altered products and crystal structure, as mentioned above. It is widely known that enstatite has been more strongly affected by aqueous alteration than any other silicates in chondrules. Thus, clarification of the alteration mechanism of enstatite would provide the information about conditions at the earliest stage of aqueous alteration processes of chondrules.

I have carried out low-temperature (100-300°C) hydrothermal experiments of enstatite and investigated the effects of experimental temperature, pH and composition of aqueous solution, duration time, polymorph and crystal structure. I here present the results of the experiments. My purposes are to investigate the altered products and altered textures of enstatite and to unravel the alteration mechanism of enstatite in order to infer the alteration conditions of chondrules.

Chapter 2

Experimental Procedures

2.1 Starting Materials

Starting materials for hydrothermal experiments were prepared as follows:

Single crystals of orthoenstatite were synthesized by the flux method (Ozima, 1982). MgO and SiO₂ powders were calculated stoichiometrically and weighted critically. The powders were added to the flux of Li₂CO₃, MoO₃, and V₂O₅ that was mixed in the proportion of 34.3, 55.8, and 9.9 wt%, respectively. The weight ratio of the powders to the flux was 0.05. Table 2.1 shows an example of synthesis data for orthoenstatite. The mixture of powders and flux was heated in a platinum crucible at 975°C for 100 hours in the air, then cooled to 700°C at cooling rate of 0.6°C/h and to room temperature at 30°C/h (Fig. 2.1). Synthesized orthoenstatite crystals were separated from the solvent by washing in hot water. The orthoenstatite single crystals range in size from 0.5 to 1.5 mm (Fig. 2.2a). Some crystals were analyzed by the Rigaku x-ray powder diffractometer (XRD) with Cu-K α radiation, installed at the Department of Chemistry, Kobe University, operating at 30 kV, 16 mA, and they were confirmed to be orthoenstatite (Fig. 2.2b).

Table 2.1: Example of orthoenstatite synthesis data.

Flux	Li ₂ CO ₃	6.14106 g
	MoO ₃	10.00000 g
	V ₂ O ₅	1.77140 g
Nutrient	MgO	0.36098 g
	SiO ₂	0.53813 g
Crucible size		20 ml
Mg/Si		1.0
Nutrient/flux		5.0 wt%
Soaking temperature		975°C
Soaking time		100 hours

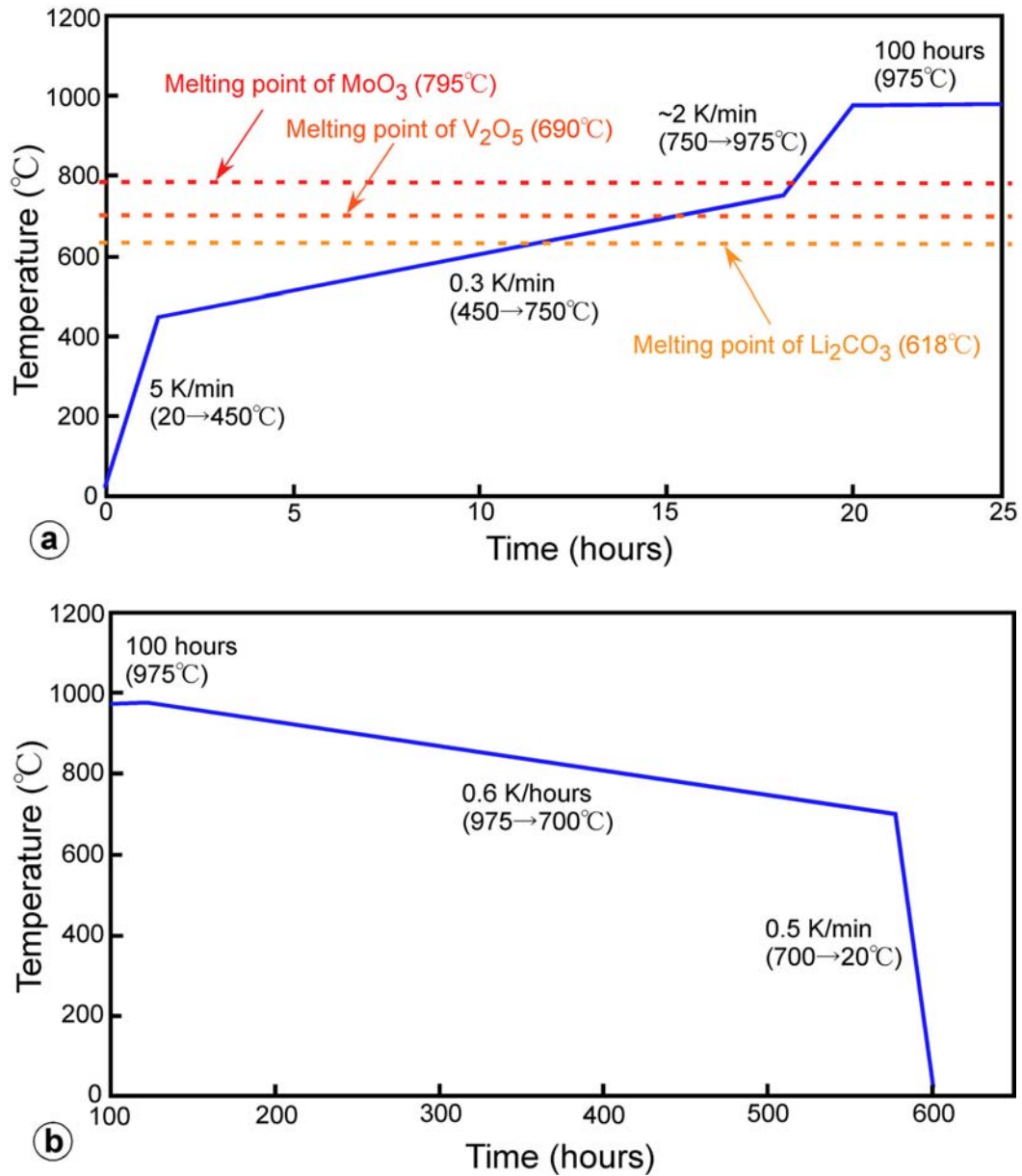


Figure 2.1: Schematic heating (a) and cooling (b) profiles of orthoenstatite synthesis by the flux method.

Single crystals of clinoenstatite were obtained by quenching after orthoenstatite has been heated at 1200°C for 48 hours. They were confirmed to be clinoenstatite by XRD (Fig. 2.2d). The crystals, ranging in size from 0.3 mm to 1.0 mm, contain many fractures and cracks (Fig 2.2c). They appear pale green in color under reflected light, suggesting that they also contain abundant twin lamellae.

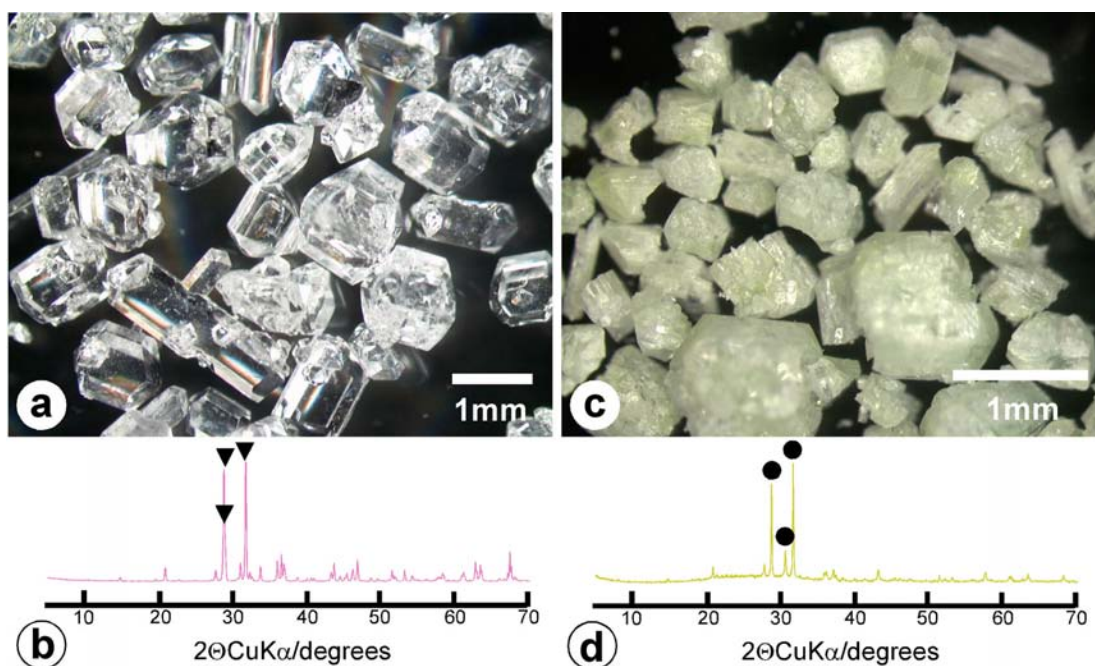


Figure 2.2: Photographs (a, c) and x-ray diffraction (XRD) patterns (b, d) of starting materials. a, b: orthoenstatite, c, d: clinoenstatite. ▼: the strongest three XRD peaks of orthoenstatite, ●: those of clinoenstatite.

Powders of orthoenstatite were obtained by grinding synthesized orthoenstatite crystals with an agate mortar. The powdered orthoenstatites range in size from 1 to 10 μm .

2.2 Hydrothermal Experiments

Three series of hydrothermal experiments were performed under the following conditions:

Experiment 1: Orthoenstatite powders were hydrothermally altered with various aqueous solution, including 1N-HCl, 1N-NaCl solution, H₂O, 0.01N-, 0.1N-, and 1N-NaOH solution, at 100, 200, and 300°C. The experiments at temperatures lower than 200°C were performed with a Teflon reaction cell of 4 ml loaded into a stainless vessel (Fig. 2.3). In each run orthoenstatite powders 50 mg were placed on the bottom of the cell and a solution 2 ml was added (*i.e.*, solution/powder ~ 40 weight ratio). The runs were performed under autogeneous water vapor pressure. For the experiments at 300°C, an autoclave (the Nikki-Soh hydrothermal apparatus HTU1-NK-H25-II) was used (Fig. 2.4). In each run orthoenstatite powders 30 mg were sealed with a solution 0.1 ml in a gold capsule (*i.e.*, solution/powder ~ 3.3 weight ratio). The capsules were loaded into an autoclave, then heated at 300°C and 1 kbar. Runs were performed for 24, 72, 168, and 336 hours. I measured the pH values of aqueous solution by pH meter at room temperature before each run and regarded the values as initial pH values for each run. The pH values of 1N-HCl, 1N-NaCl solution, H₂O, 0.01N-, 0.1N-, and 1N-NaOH solution are approximately 0, 6, 7, 12, 13, and 14, respectively. The experimental conditions are summarized in Table 2.2.

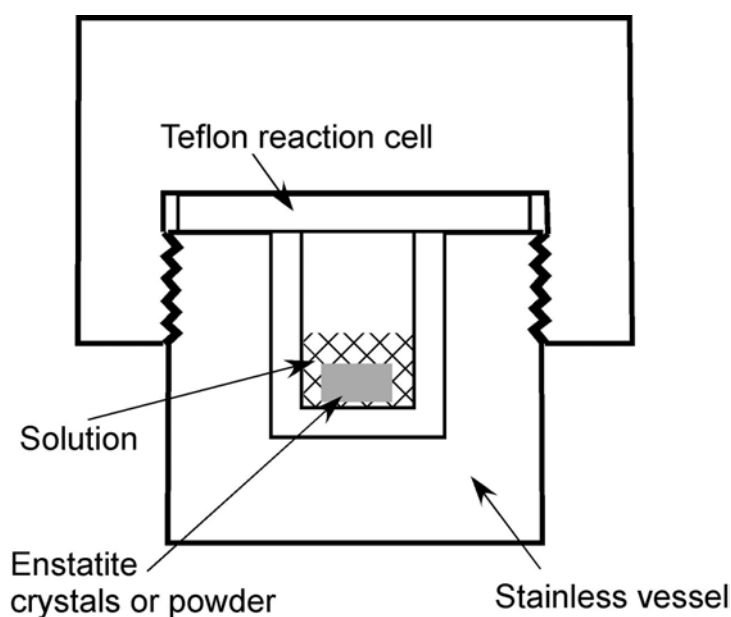


Figure 2.3: Schematic diagram of a Teflon reaction cell loaded in a stainless vessel.

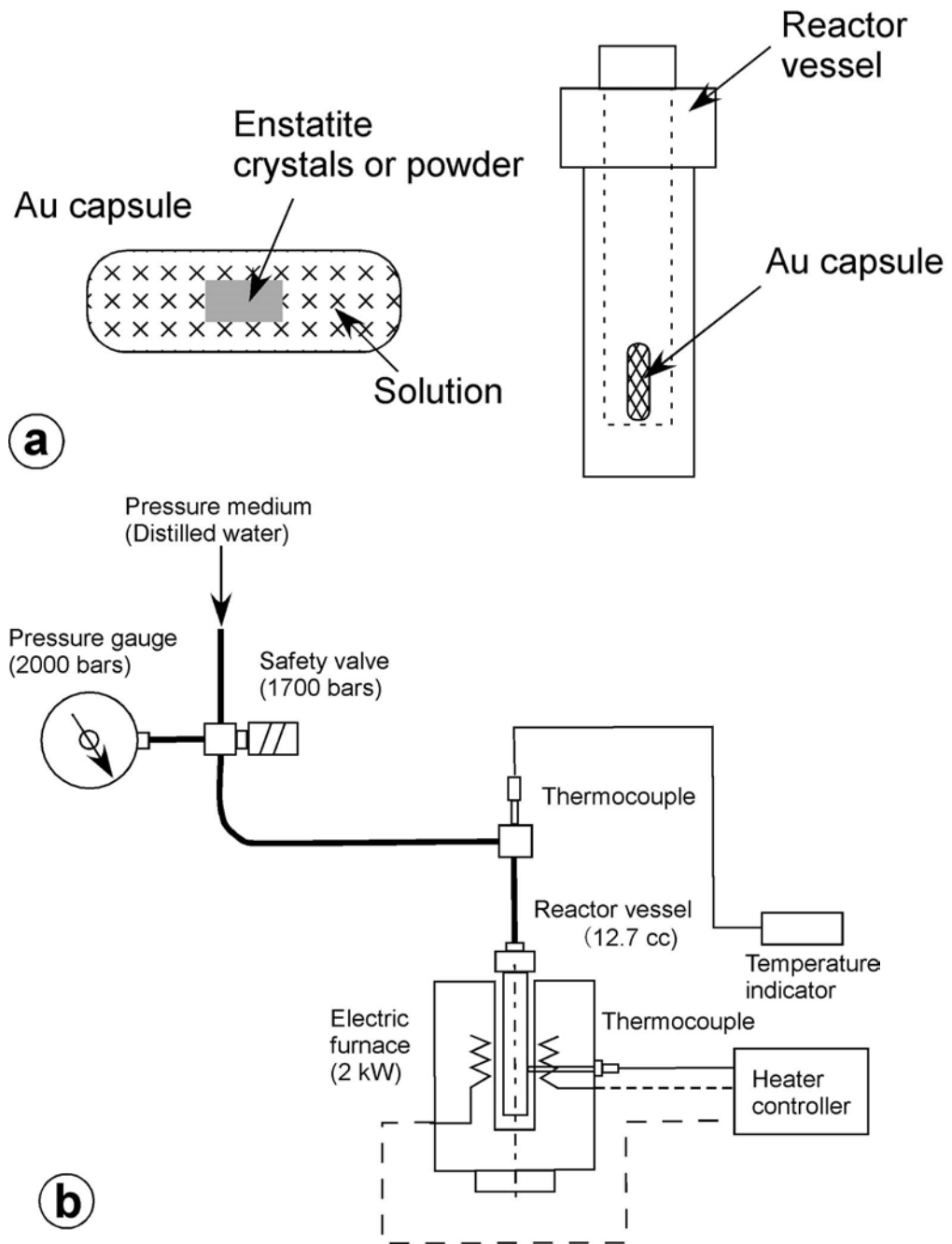


Figure 2.4: Schematic diagrams of a charge (a) and hydrothermal apparatus (b).

Table 2.2: Experimental conditions and products for *Experiment 1*.

Starting material	Solution		Temperature (°C)	Time (hours)	Products ^a
OEn powder	HCl	1N	200	72	No change
OEn powder	HCl	1N	300	24	No change
OEn powder	HCl	1N	300	168	No change
OEn powder	HCl	1N	300	336	No change
OEn powder	NaCl	1N	200	168	No change
OEn powder	NaCl	1N	300	168	No change
OEn powder	H ₂ O		100	168	No change
OEn powder	H ₂ O		200	168	No change
OEn powder	H ₂ O		200	336	No change
OEn powder	H ₂ O		300	24	No change
OEn powder	H ₂ O		300	72	No change
OEn powder	H ₂ O		300	168	Srp
OEn powder	H ₂ O		300	336	Srp
OEn powder	NaOH	0.01N	200	168	No change
OEn powder	NaOH	0.01N	300	168	Srp
OEn powder	NaOH	0.1N	200	168	Srp
OEn powder	NaOH	0.1N	300	168	Srp+Smec
OEn powder	NaOH	1N	100	168	No change
OEn powder	NaOH	1N	100	336	No change
OEn powder	NaOH	1N	200	24	Srp
OEn powder	NaOH	1N	200	72	Srp
OEn powder	NaOH	1N	200	168	Srp+Smec
OEn powder	NaOH	1N	300	24	Srp+Smec
OEn powder	NaOH	1N	300	72	Srp+Smec
OEn powder	NaOH	1N	300	168	Srp+Smec
OEn powder	NaOH	1N	300	336	Srp+Smec

The experiments at 100 and 200°C were performed under autogeneous water vapor pressure, while those at 300°C were performed under pressure of 1 kbar.

^a identified by XRD; Srp=Serpentine, Smec=Smectite

Experiment 2: Orthoenstatite powders mixed with Fe powders were hydrothermally altered with 1N-NaOH solution at 300°C in the weight ratio of orthoenstatite: Fe as 9: 1, and 5: 5. For 9: 1, orthoenstatite powders 27 mg and Fe powders 3 mg were sealed with a solution 0.1 ml in a gold tube (*i.e.*, solution/powder ~ 3.3 weight ratio). For 5: 5, orthoenstatite powders 15 mg and Fe powders 15 mg were sealed with a solution 0.1 ml in a gold capsule (*i.e.*, solution/powder ~ 3.3 weight ratio). These capsules were loaded into an autoclave, then heated at 300°C and 1 kbar. Runs were performed for 168 hours. The experimental conditions are summarized in Table 2.3.

Table 2.3: Experimental conditions and products for *Experiment 2*.

Starting materials ^a		Solution	Products ^{b,c}
OEn powder	Fe powder		
10	0	NaOH 1N	Srp+Smec (Srp=Smec)
9	1	NaOH 1N	Srp+Smec (Srp=Smec)
5	5	NaOH 1N	Srp+Smec (Srp>Smec)

All experiments were performed at 300°C, 1 kbar for 168 hours.

^a Weight ratio.

^b identified by XRD; Srp=Serpentine, Smec=Smectite.

^c ()=Relative amount of the products estimated by XRD.

Experiment 3: Orthoenstatite crystals or clinoenstatite crystals, mixed with Fe powders, were hydrothermally altered with H₂O or 1N-NaOH solution at 300°C. In each run the crystals 15 mg and Fe powders 15 mg were sealed with a solution 0.05 ml in a gold capsule (*i.e.*, solution/crystals ~ 1.7 weight ratio). The capsules were loaded into an autoclave, then heated at 300°C and 100 bars. Runs were performed for 168 hours. The experimental conditions are summarized in Table 2.4.

Table 2.4: Experimental conditions and products for *Experiment 3*.

Starting materials		Solution	Products ^a
OEn crystals	Fe powder		
CEn crystals	Fe powder	H ₂ O	Srp
OEn crystals	Fe powder	NaOH 1N	Srp
CEn crystals	Fe powder	NaOH 1N	Srp

All experiments were performed at 300°C, 100 bars for 168 hours

^a identified by XRD; Srp=Serpentine, Smec=Smectite

2.3 Characterization of Products

The samples recovered from *Experiment 1* and *2* were analyzed by XRD, operating 30 kV and 16 mA. In order to identify smectite, an ethylene glycol treatment was conducted for some samples.

Thin sections were made from the samples recovered from *Experiment 3*. They were studied by using an optical microscope, and a scanning electron microscope (SEM) (JEOL JSM-5800) equipped with an energy dispersive X-ray spectrometer (EDS). EDS analyses were obtained at 15 kV and 0.4 nA. Data corrections were made by the Phi-Rho-Z method. Well-characterized natural and synthetic minerals and glasses were used as standards. For the analysis, we used focused electron beam of $\sim 2 \mu\text{m}$ in diameter. Some samples were further examined by a transmission electron microscope (TEM) (JEOL JEM-2010) equipped with EDS, operated at 200 kV.

Chapter 3

Results: Hydrothermal products and textural characteristics of altered enstatite

3.1 Results of *Experiment 1*

Phyllosilicates were produced in 12 runs from a total of 26 runs (Table. 2.2). They consist of two assemblages: serpentine and serpentine + smectite. The XRD peaks of 0.73~0.75 nm (*002* reflection) and 0.362~0.365 nm (*004* reflection) are derived from serpentine, whereas those of 1.31~1.41 nm (*001* reflection), which were transferred to about 1.74 nm by an ethylene glycol treatment, about 0.3065 nm (*005* reflection), and about 0.1527 nm (*060* reflection) are smectite. I could recognize that the assemblages of phyllosilicates (*i.e.*, no phyllosilicate, serpentine, and serpentine + smectite) were affected by pH and composition of aqueous solution, experimental temperature, and duration time as follows.

3.1.1 pH and composition of aqueous solution

Figure 3.1 shows the XRD patterns of orthoenstatite altered with various solutions, including 1N-HCl, 1N-NaCl solution, H₂O, 0.01N-, 0.1N-, 1N-NaOH solution, at 300°C and 1 kbar for 168 hours as well as that of unaltered orthoenstatite. Both serpentine and smectite were produced in the solution with 0.1N-NaOH and 1N-NaOH (Figs. 3.1F-G). The peaks of orthoenstatite treated with 0.1N- and 1N-NaOH solutions appear to be weaker compared with those of unaltered orthoenstatite, suggesting that serpentine and smectite grew by the consumption of orthoenstatite. Qualitative analyses by TEM-EDS reveal that, serpentine produced in the present experiments is enriched with O, Mg, and Si, whereas smectite is enriched with O, Si, Mg, and Na. The ideal chemical formulae of Mg-endmember serpentine and Mg-smectite (saponite) are Mg₃Si₂O₅(OH)₄ and Na_{0.33}Mg₃(Si_{3.67}, Al_{0.33})O₁₀(OH)₂**n*H₂O, respectively. Produced serpentine probably has

ideal chemical formula, whereas produced smectite does not so because the system in the present experiments did not include Al. The chemical formula of the smectite could not be understood with accuracy, but it may approximate that of Na-bearing talc $[\text{Mg}_3\text{Si}_4\text{O}_{10}(\text{OH})_2]$. The XRD peaks of serpentine and, in particular, smectite produced from 1N-NaOH solution are stronger than those from 0.1N-NaOH solution, suggesting that the phyllosilicates tend to form under high pH and Na-rich condition as discussed below. Weak XRD peaks of serpentine are found in the run products of orthoenstatite with 0.01N-NaOH solution and H_2O , although no peaks of smectite are found (Figs. 3.1D-E). No change in the mineral assemblage was observed in the products with 1N-HCl and 1N-NaCl solution (Figs. 3.1B-C).

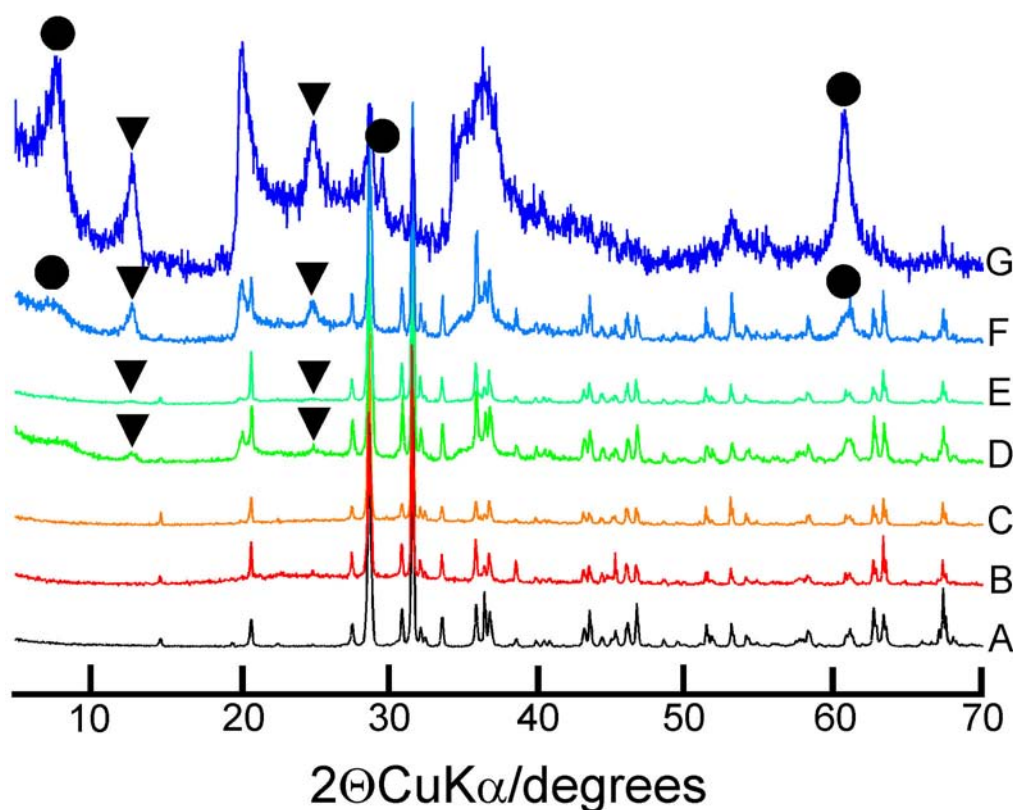


Figure 3.1: X-ray diffraction patterns of orthoenstatite unaltered and those altered with various solution at 300°C and 1 kbar for 168 hours. A: unaltered; B: 1N-HCl; C: 1N-NaCl solution; D: H_2O ; E: 0.01N-NaOH solution; F: 0.1N-NaOH solution; G: 1N-NaOH solution. ▼: serpentine, ●: smectite.

3.1.2 Experimental temperature

The XRD patterns of orthoenstatite altered with H₂O (Fig. 3.2), 1N-NaOH solution (Fig. 3.3) at 100, 200, and 300°C for 168 hours are shown as well as those of unaltered orthoenstatite. Weak XRD peaks of serpentine were found in the run products from H₂O at 300°C, whereas no change in the mineral assemblage was observed at 100 and 200°C (Fig. 3.2). In the run products from 1N-NaOH solution, the XRD peaks of both serpentine and smectite were recognized at 200 and 300°C, whereas no change was observed at 100°C (Fig. 3.3). Moreover, the XRD peaks of the phyllosilicates at 300°C were stronger than those at 200°C. These results suggest that the phyllosilicates tend to be produced at higher temperature in the range of present experimental temperature.

Figure 3.4 shows the XRD patterns of orthoenstatite altered with 0.1N-NaOH solution at 200 and 300°C for 168 hours as well as that of unaltered orthoenstatite. The assemblages of produced phyllosilicates differed between different experimental temperatures. At 200°C, the presence only of serpentine was recognized, whereas, at 300°C, the presence of both serpentine and smectite was recognized. The result suggests that smectite tends to be produced at higher temperature compared with serpentine.

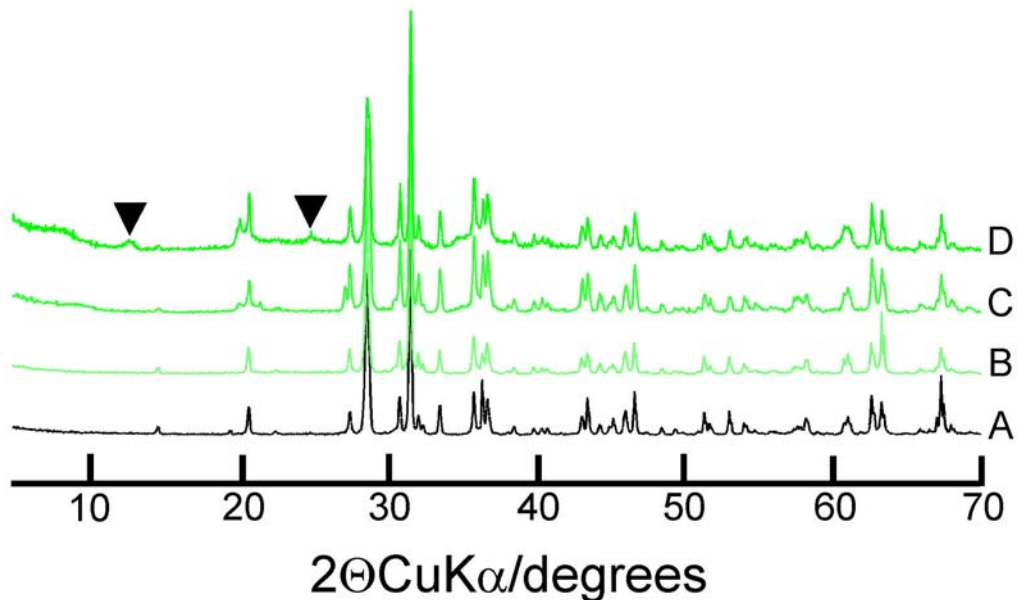


Figure 3.2: X-ray diffraction patterns of orthoenstatite unaltered and those altered with H₂O at 100, 200, and 300°C for 168 hours. A: unaltered; B: 100°C; C: 200°C; D: 300°C. ▼: serpentine.

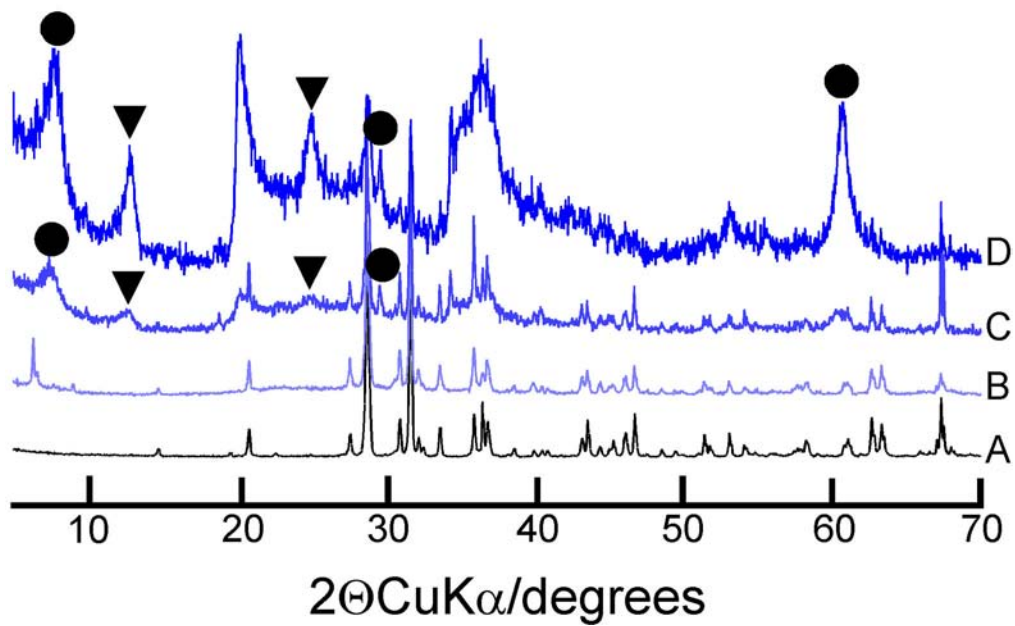


Figure 3.3: X-ray diffraction patterns of orthoenstatite unaltered and those altered with 1N-NaOH solution at 100, 200, and 300°C for 168 hours. A: unaltered; B: 100°C; C: 200°C; D: 300°C. ▼: serpentine, ●: smectite.

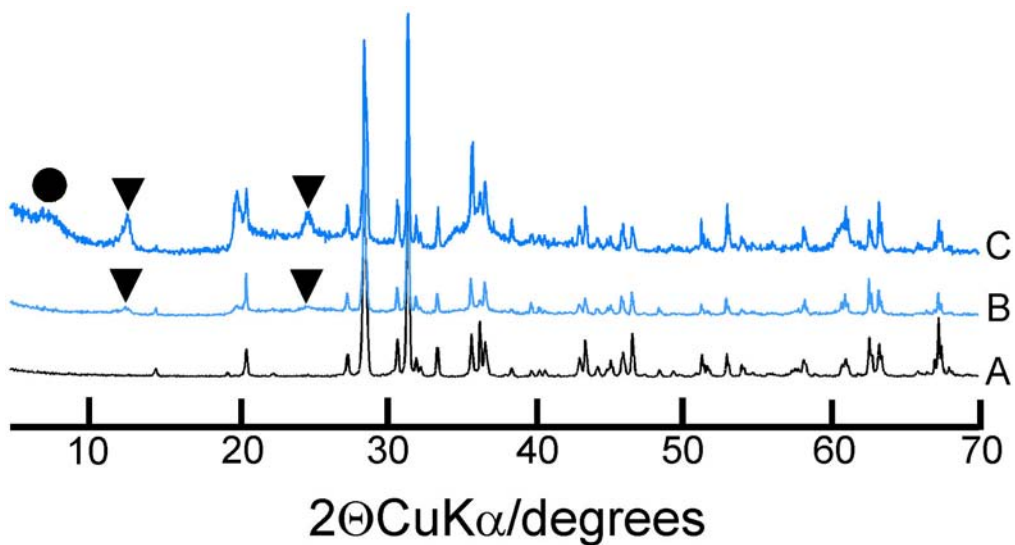


Figure 3.4: X-ray diffraction patterns of orthoenstatite unaltered and those altered with 0.1N-NaOH solution at 200, and 300°C for 168 hours. A: unaltered; B: 200°C; C: 300°C. ▼: serpentine, ●: smectite.

3.1.3 Duration time

The XRD patterns of orthoenstatite altered with 1N-NaOH solution at 200 (Fig. 3.5) and 300°C (Fig. 3.6) for 24, 72, 168, and 336 hours are shown as well as those of unaltered orthoenstatite (Duration time of 336 hours was from only the experiment at 300°C). At 300°C, the presence of both serpentine and smectite was recognized for all duration time in the present experiments, although the XRD peaks of the phyllosilicates for 24 hours were weaker compared with those for the duration time above 72 hours. At 200°C, the presence only of serpentine was recognized for 24 and 72 hours, whereas the presence of both serpentine and smectite was recognized for 168 hours. The result suggests that serpentine firstly crystallized in the solution with 1N-NaOH and smectite subsequently crystallized in the residue solution.

Figure 3.7 summarizes the T-T-T diagram of the produced phyllosilicates from orthoenstatite with 1N-NaOH solution. This diagram shows that, under alkaline condition, serpentine + smectite would be more stable as the assemblage of phyllosilicates compared with only serpentine. At lower temperature (200°C) and shorter duration time (24 and 72 hours), only serpentine probably appeared as a maetastable phase.

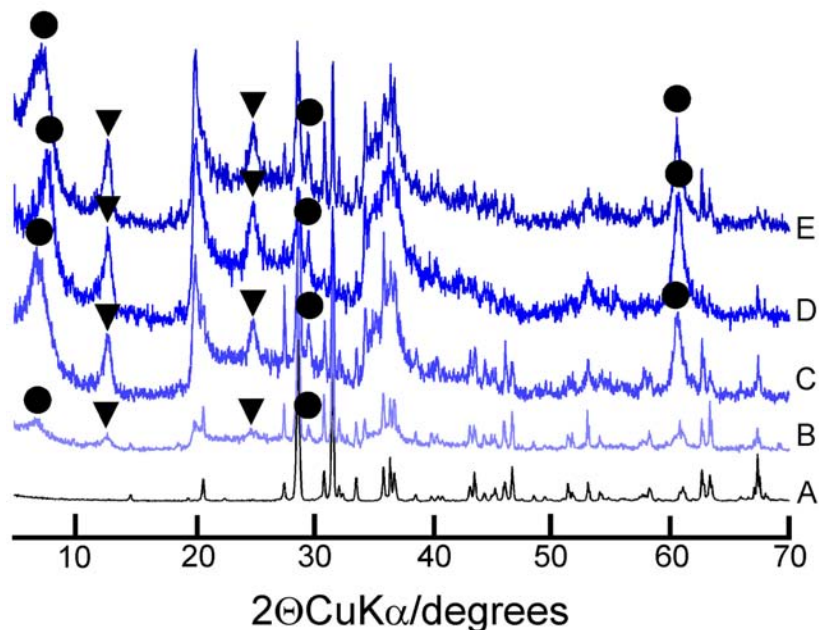


Figure 3.5: X-ray diffraction patterns of orthoenstatite unaltered and those altered with 1N-NaOH solution at 300°C for 24, 72, 168, 336 hours. A: unaltered; B: 24 hours; C: 72 hours; D: 168 hours; E: 336 hours. ▼: serpentine, ●: smectite.

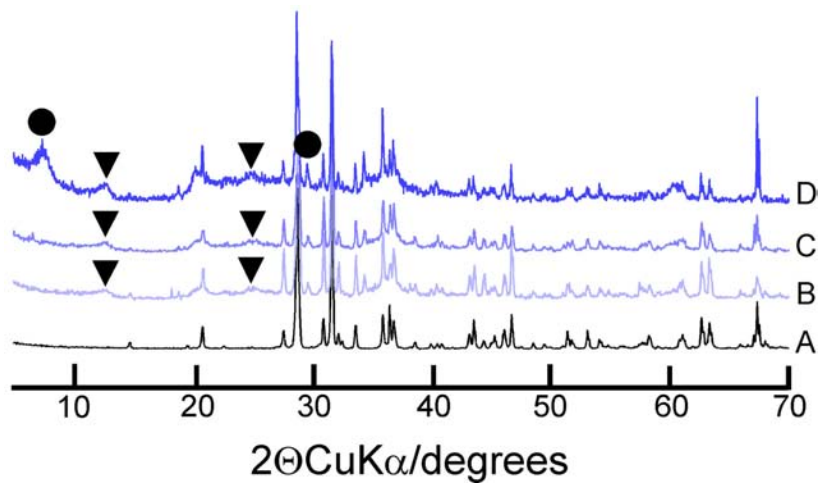


Figure 3.6: X-ray diffraction patterns of orthoenstatite unaltered and those altered with 1N-NaOH solution at 200°C for 24, 72, 168 hours. A: unaltered; B: 24 hours; C: 72 hours; D: 168 hours. ▼: serpentine, ●: smectite.

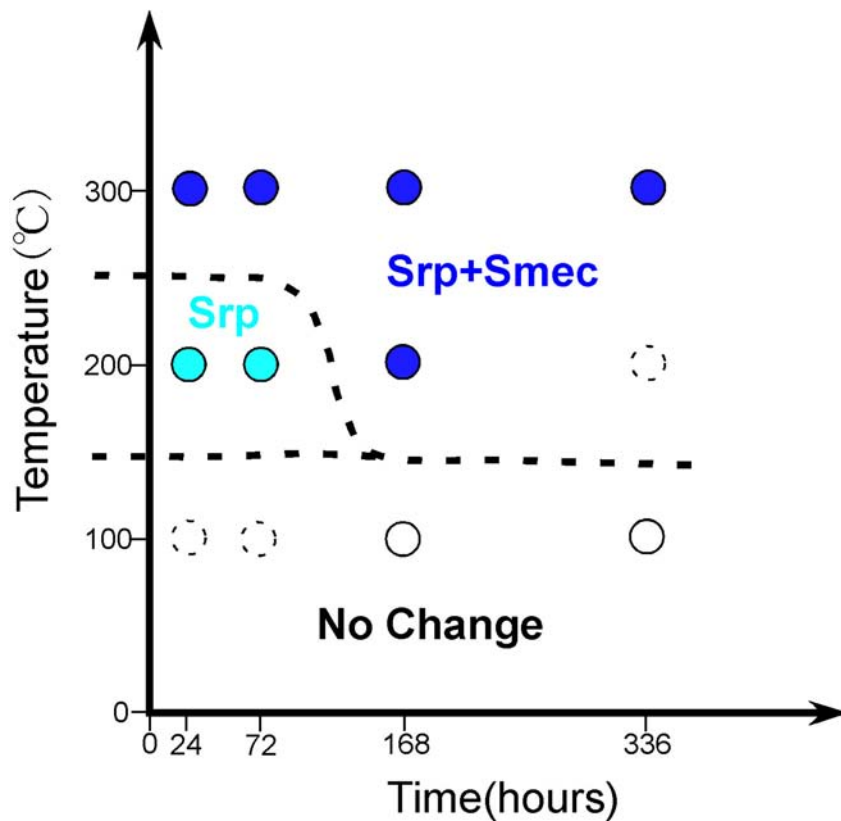


Figure 3.7: T-T-T diagram of the produced phyllosilicates from orthoenstatite altered with 1N-NaOH solution. Circles show the experimental points. Srp: serpentine; Smec: smectite.

3.1.4 Summary

Figure 3.8 summarizes the results of *Experiment 1*. From this figure, I can say that (a) Under neutral and alkaline condition, serpentine tends to be produced, whereas, under only strong alkaline condition, smectite tends to be produced. (b) Simultaneously, smectite tends to be produced along with the advanced high temperature compared with serpentine.

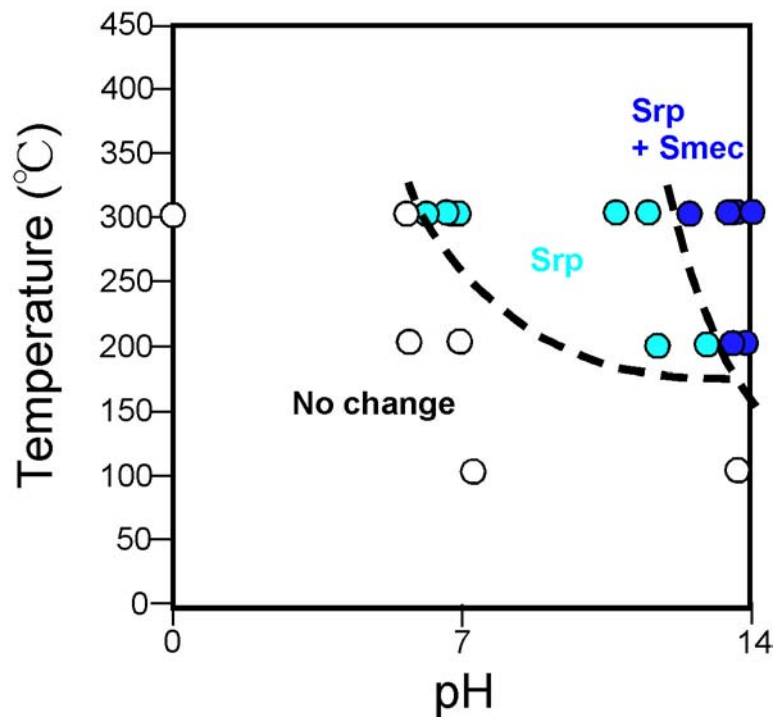


Figure 3.8: Schematic diagram of the results of *Experiment 1*. Circles show the experimental points. Srp: serpentine; Smec: smectite.

3.2 Results of *Experiment 2*

Phyllosilicates were also produced from the hydrothermal experiments on the mixtures of orthoenstatite and Fe powder with 1N-NaOH solution. The assemblage of produced phyllosilicate was serpentine + smectite, but the proportion of serpentine to smectite depends on the Fe content. Figure 3.9 shows the XRD patterns of orthoenstatite mixed with Fe altered with 1N-NaOH solution at 300°C and 1 kbar for 168 hours in the weight ratio of orthoenstatite: Fe as 10: 0 (Fig. 3.9A), 9: 1 (Fig. 3.9B), and 5: 5 (Fig. 3.9C). In the case of the weight ratio of orthoenstatite: Fe as 10: 0 and 9: 1 (proportion of Fe content is low), the XRD peaks of serpentine show similar strength as those of smectite. In the case of the weight ratio of orthoenstatite: Fe as 5: 5 (proportion of Fe content is relatively high), the XRD peaks of serpentine appear distinctly stronger than those of smectite. The result suggests that serpentine tends to be produced along with the advanced Fe content.

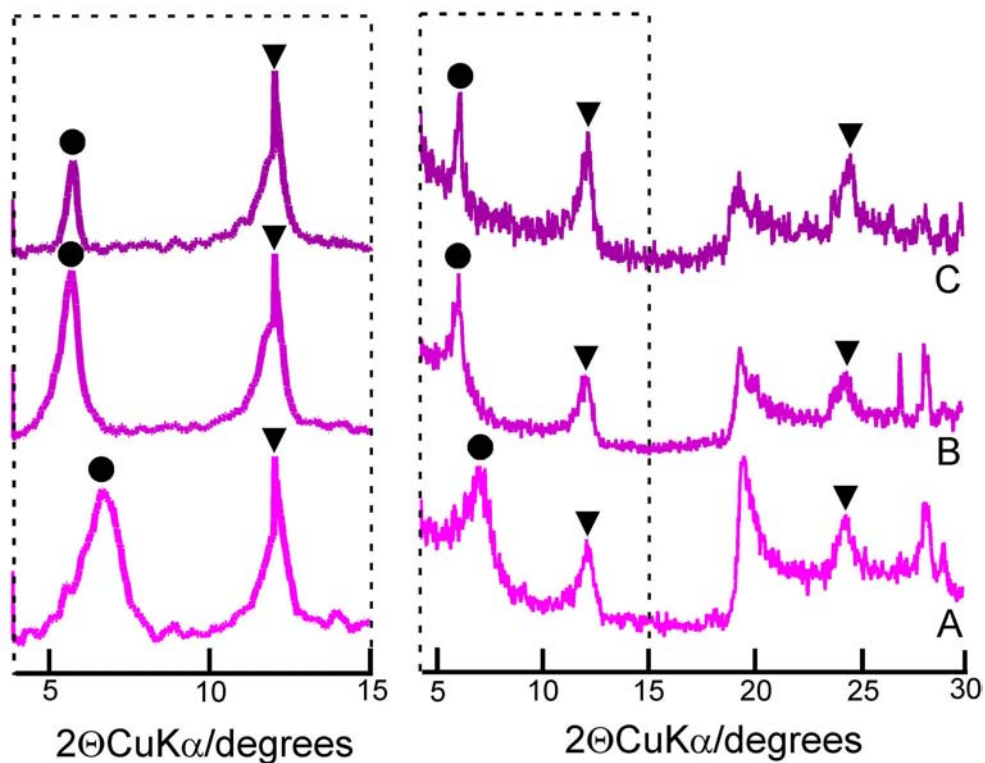


Figure 3.9: X-ray diffraction patterns of orthoenstatite powders mixed with Fe powders altered with 1N-NaOH solution at 300°C for 168 hours in the weight ratio of orthoenstatite: Fe as 10: 0 (A), 9: 1 (B), 5: 5 (C). Right diagrams show the raw data and left diagrams show the disposed results (after smoothing, elimination of background, and stripping of K-alpha-2). ▼: serpentine, ●: smectite.

3.3 Results of *Experiment 3*

3.3.1 SEM Analysis

Crystals of enstatite are partially altered to phyllosilicate. The phyllosilicate has composition similar to Fe-bearing serpentine (Fig. 3.10). Backscattered electron (BSE) images revealed that there is a difference in the degree of alteration by serpentine between orthoenstatite and clinoenstatite treated with the same solution. In the case of orthoenstatite, serpentine partially replaces only the margin of orthoenstatite crystals to large extents, thus forming thicken rims (5-15 μm in thickness) (Figs. 3.11a-b). In the case of clinoenstatite, serpentine partially replaces clinoenstatite crystals along the margins like as the case of orthoenstatite and further along fractures that occur throughout the crystals, forming a mesh-like structure (Figs. 3.11c-d). So, the crystals of clinoenstatite appear to be more highly altered than those of orthoenstatite treated with the same solution.

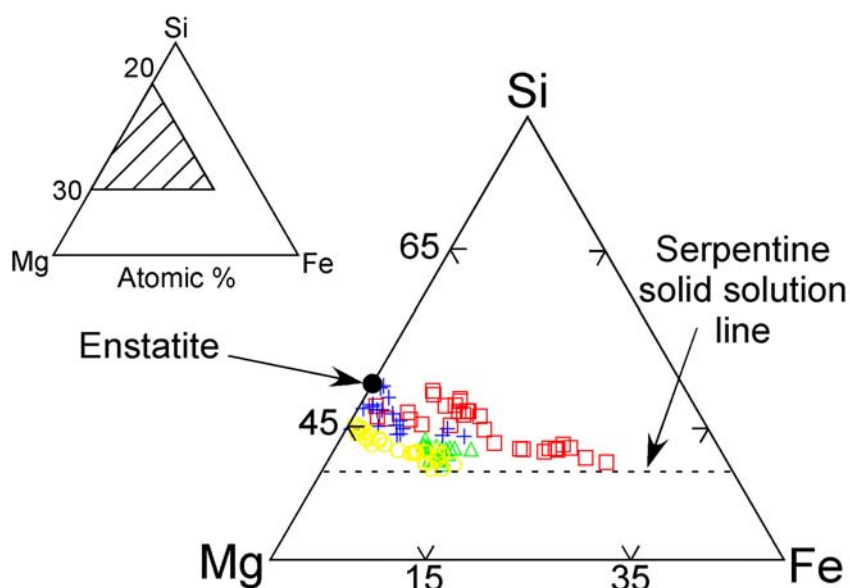


Figure 3.10: EDS analyses of phyllosilicate produced by *Experiment 3* in terms of atomic percents of Si, Mg and Fe. Also shown is the ideal solid solution line of serpentine ($(\text{Mg}, \text{Fe})_3\text{Si}_2\text{O}_5(\text{OH})_4$). \square : orthoenstatite altered with H_2O ; \triangle : orthoenstatite altered with 1N-NaOH solution; $+$: clinoenstatite altered with H_2O ; \circ : clinoenstatite altered with 1N-NaOH solution.

There is also a difference in the degree of alteration by serpentine between H_2O

and 1N-NaOH solution using the same starting material. For instance, the thickness of serpentine rims at the margins of orthoenstatite crystals treated with 1N-NaOH solution is thicker than that at the margins of orthoenstatite crystals treated with H₂O (Fig. 3.11b vs. 3.11a). The result suggests that phyllosilicates tend to be easy to develop under alkaline condition. It is consistent with the results of *Experiment 1*.

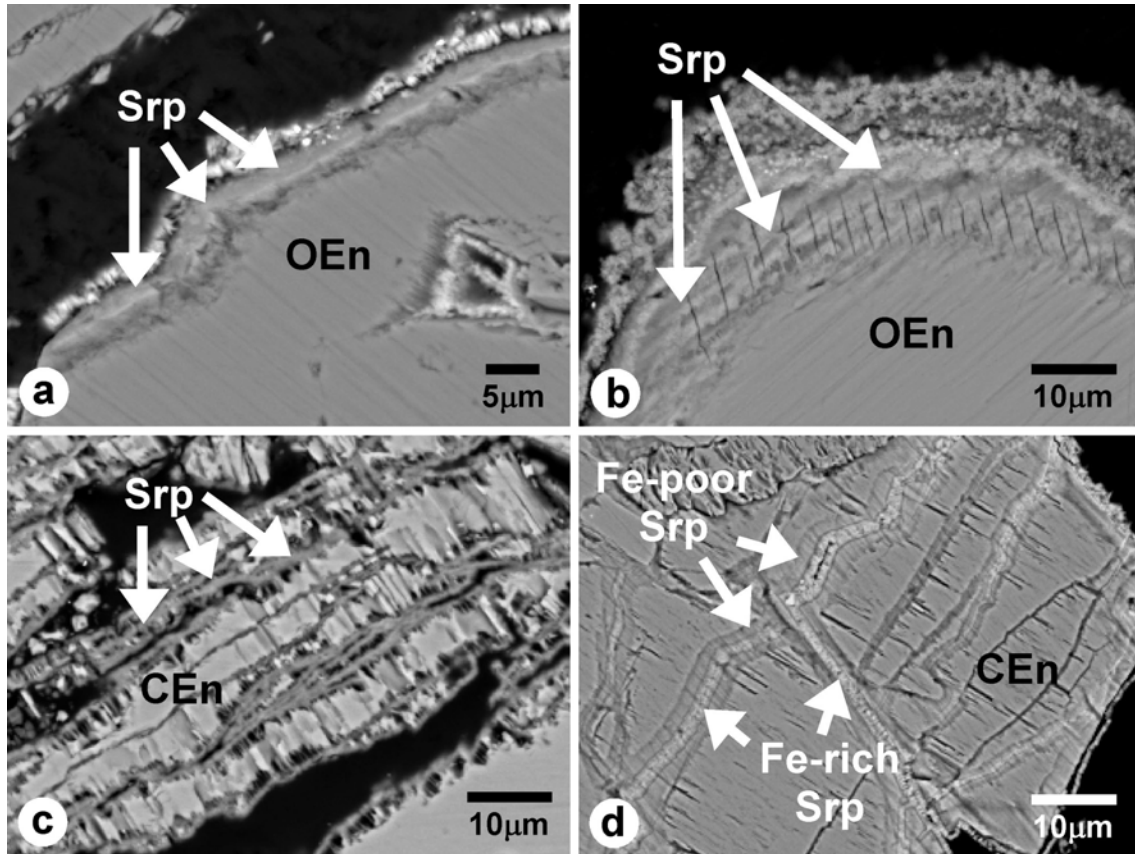


Figure 3.11: Backscattered electron images of the portion of the recovered samples from *Experiment 3*. (a) orthoenstatite altered with H₂O; (b) orthoenstatite altered with 1N-NaOH solution; (c) clinoenstatite altered with H₂O; (d) clinoenstatite altered with 1N-NaOH solution. OEn: orthoenstatite; CEn: clinoenstatite; Srp: serpentine.

Serpentines produced by clinoenstatite altered with 1N-NaOH solution can be divided to two types (Fig. 3.11d): one occurs as rims replacing clinoenstatite grains, while the other occurs as veins. In backscattered electron images, the veins are distinctly brighter relative to the rims (Fig. 3.11d). EDS analyses revealed that serpentine in rims is poor in Fe ($Fe/(Mg+Fe) < 0.08$), while serpentine in veins is rich in Fe ($Fe/(Mg+Fe) = 0.1-0.21$). It is obvious that Fe-poor serpentine had been formed along with the inner walls of fractures at first and then Fe-rich serpentine has sealed the extra spaces of the

fractures. In order to reveal the morphology and crystallographic characteristics of two types of serpentine, I performed TEM analysis of the samples as described below.

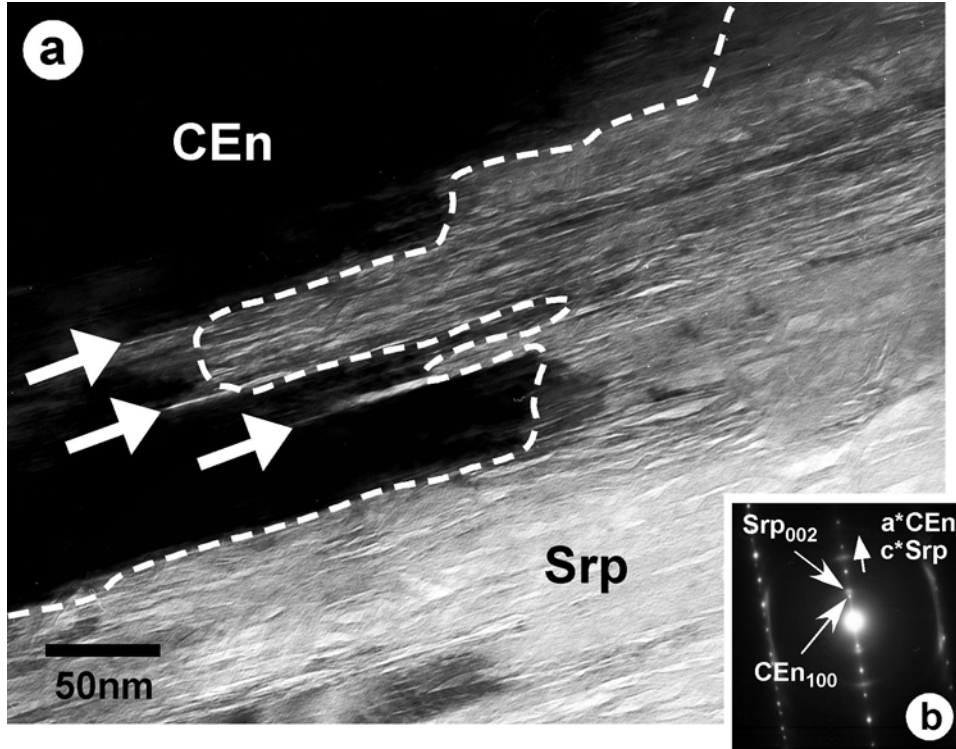


Figure 3.12: TEM image (a) and SAED pattern (b) of the boundary between clinoenstatite and Fe-poor serpentine in the recovered sample from *Experiment 3*. Fe-poor serpentine directly replaces clinoenstatite and appear to be preferentially formed along with twin lamellae (white broad arrows). SAED pattern shows that c^* axis of serpentine is approximately parallel to a^* of clinoenstatite.

3.3.2 TEM analysis

The high-resolution TEM (HRTEM) observations revealed that Fe-poor serpentine occurs as relatively large (~1000 nm in size), platy, fibrous crystal. Serpentine directly replaces clinoenstatite and appears to be preferentially formed along with twin lamellae (Fig. 3.12). Selected area electron diffraction (SAED) patterns revealed that c^* axis of serpentine is approximately parallel to a^* axis of clinoenstatite (Fig. 3.12), suggesting that two minerals have topotactic relationship to each other. On the other hands, Fe-rich serpentine is small (<500 nm in size), curved, fibrous crystal randomly oriented (*i.e.*, non-topotactic) (Fig. 3.13). In places, Fe-rich serpentine shows incomplete polygonal texture (Fig. 3.14). Fe-poor serpentine tends to show higher crystallinity than Fe-rich serpentine, because the former is stronger to damage by the electron beam in TEM

observations compared with the latter.

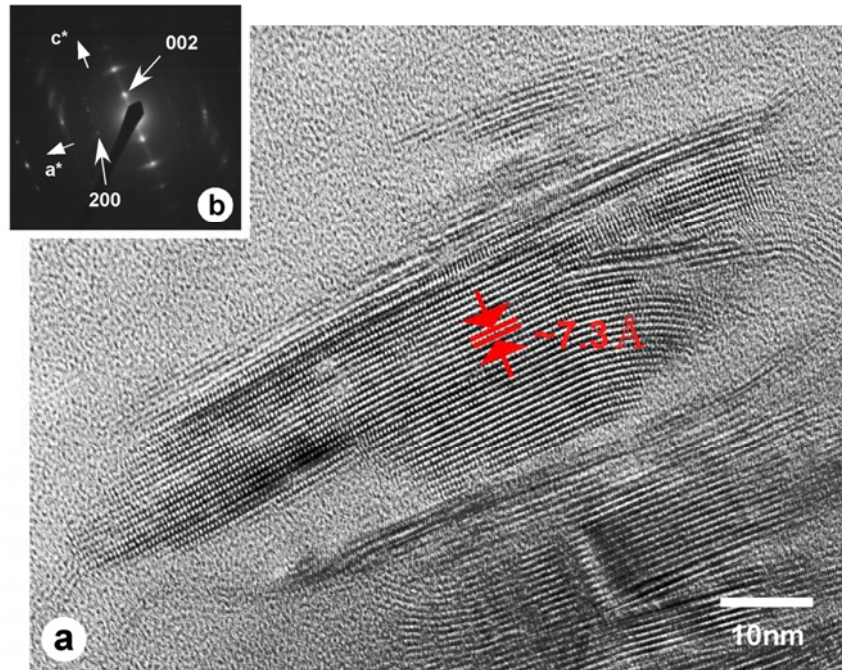


Figure 3.13: High-resolution TEM (HRTEM) image (a) and selected area electron diffraction (SAED) pattern (b) of Fe-rich serpentine in the recovered sample from *Experiment 3*.

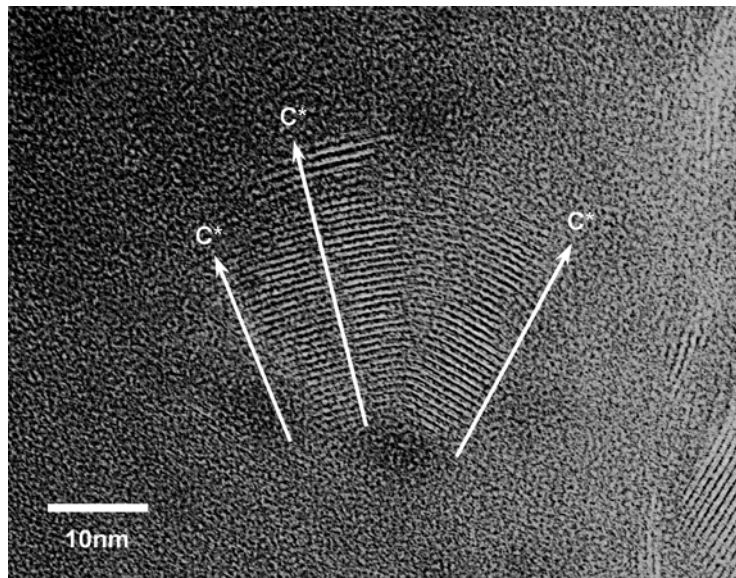


Figure 3.14: High-resolution TEM (HRTEM) image of Fe-rich serpentine in the recovered sample from *Experiment 3*. Note that, in places, Fe-rich serpentine shows incomplete polygonal texture.

Chapter 4

Discussion: Alteration mechanism of enstatite and aqueous alteration processes of chondrites

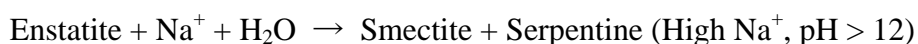
4.1 Products of Experiments

The secondary mineral assemblages obtained from hydrothermal experiments of enstatite consist of two types: serpentine and serpentine + smectite, depending on pH and composition of aqueous solutions, experimental temperature (*Experiment 1*) and the Fe content mixed with enstatite (*Experiment 2*). Figure 3.8 shows that the slope of boundary between serpentine and serpentine + smectite is steep, suggesting that pH and composition of aqueous solutions rather than experimental temperature must be more critical factor for the alteration mineralogy of enstatite.

4.1.1 Formation process of smectite from enstatite

Smectite, as well as serpentine, crystallized from hydrothermal experiments on enstatite with 0.1N- and 1N-NaOH solutions at 300°C, whereas no smectite crystallized from those on enstatite with 0.01N-NaOH and other solutions at the same temperature (Fig. 3.1). Measured pH values of 0.01N-, 0.1N-, and 1N-NaOH solutions are approximately 12, 13, and 14, respectively. And Na⁺ concentrations in those solutions are estimated to be about 10⁻², 10⁻¹, and 1 mol/l, respectively. The XRD peaks of the smectite obtained became distinctly strong with increasing pH value and Na⁺ concentration in aqueous solutions (Fig. 3.1). These results suggest that smectite tends to form under high pH and Na-rich conditions.

Possible alteration reaction of enstatite to smectite + serpentine is as follows:



The alteration process probably consists of three stages (Fig. 4.1). At the first stage, dissolution of enstatite by alkaline solution released Mg and Si ions into the solution.

The next was the formation only of serpentine, because, under alkaline conditions, serpentine firstly crystallized and smectite subsequently crystallized (see 3.1.3, Fig. 3.7). Under alkaline conditions ($\text{pH} > 10$), Mg ions can readily precipitate as $\text{Mg}(\text{OH})_2$ that is probably related to serpentine, whereas the solubility of SiO_2 became enhanced (Stumm and Morgan, 1996). Thus, much Mg ions and less Si ions in the solution probably reacted with enstatite to form serpentine. At the last stage, excess Si ions together with Na ions in the residue solution formed smectite.

Low availability of Na ion in aqueous solution would prevent the formation of smectite as the result of enstatite with 0.01N-NaOH solution. Sodium ion occurs as an interlayer cation in smectite crystal structure. And the cation is essentially necessary for the formation of smectite. High pH condition is also necessary for the formation of smectite. It is consistent with the results of smectite synthesis (Kloprogge et al., 1999). Torii et al. (1998) hydrothermally synthesized interstratified lizardite/saponite from the slurries prepared from Si-Al-Mg gels, NaOH, and water at 300°C . The pH of the slurries was adjusted to be in the range of 11.5-11.8.

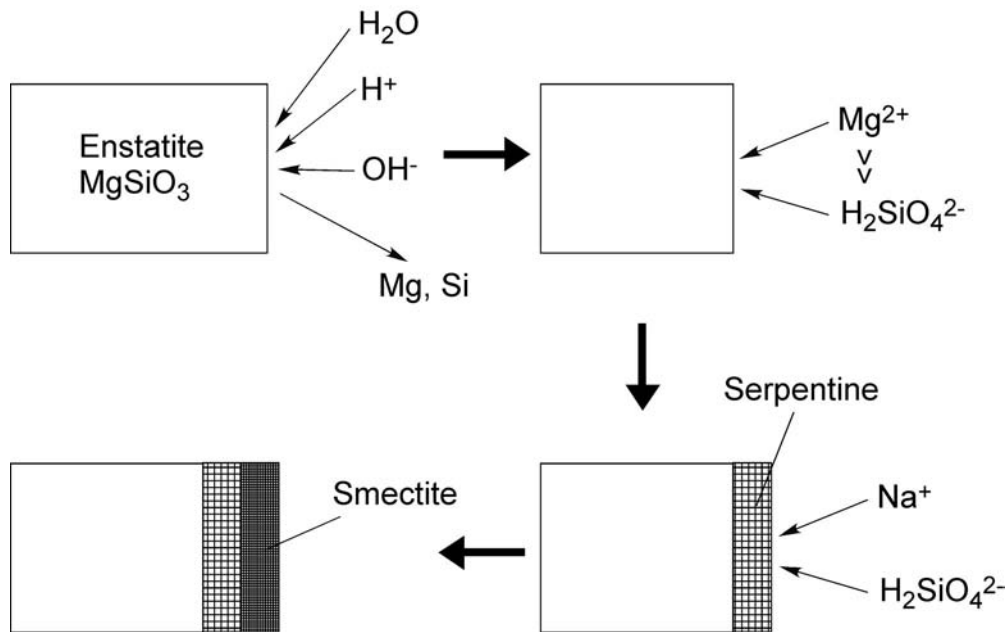
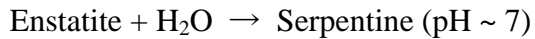


Figure 4.1: Proposed alteration process under Na-rich and high pH condition. Enstatite is dissolved by alkaline solution to release Mg and Si. Much Mg and less Si in the solution crystallize serpentine. Excess Si and Na in the residue solution crystallize smectite.

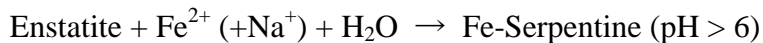
4.1.2 Formation process of serpentine from enstatite

Serpentine crystallized from enstatite with H₂O at 300°C (Fig. 3.1). The result suggests that serpentine tends to form under neutral condition, which must be unstable for smectite. The alteration reaction is probably according to



Under neutral condition, serpentine could crystallize by the reaction of enstatite with both Mg and Si ions dissolved from enstatite in aqueous solution (Fig. 4.2). It is consistent with the results of hydrothermal experiments by Martin and Fyfe (1970). They reacted enstatite with H₂O at the temperature below 400°C to obtain serpentine as well as forsterite and talc.

The results of hydrothermal experiments on the mixtures of enstatite and Fe powder with 1N-NaOH solution (*Experiment 2*) suggest that, under Fe-rich condition, serpentine rather than smectite tends to be produced even from high pH aqueous solutions enriched with Na⁺ (Fig. 3.9). Iron ions dissolved from Fe powder in alkaline solution would promote the formation of serpentine at the second stage of proposed alteration process of enstatite to smectite + serpentine (Fig. 4.3). From hydrothermal experiments on the mixtures of enstatite crystals and Fe with H₂O or 1N-NaOH solution (*Experiment 3*), the presence only of Fe-bearing serpentine was recognized under both neutral and alkaline conditions (see 3.3). Thus, in enstatite-Fe(-Na)-H₂O system, serpentine is more stable compared with smectite and the alteration reaction is probably proposed as follows:



It is widely known that serpentine can readily form by alteration of mafic silicates such as olivine under acidic to alkaline conditions (*e.g.*, Yada and Iishi, 1974; Takatori et al., 1993). Ferromagnesian cation to silicon ratios of smectite, enstatite, and serpentine are about 0.75, 1, and 1.5, respectively. Thus, alteration of enstatite to serpentine is essentially necessary for the addition of ferromagnesian ions to the system. Enstatite-Fe(-Na)-H₂O system must achieve the condition enriched with ferromagnesian ions to promote the formation of serpentine rather than that of smectite.

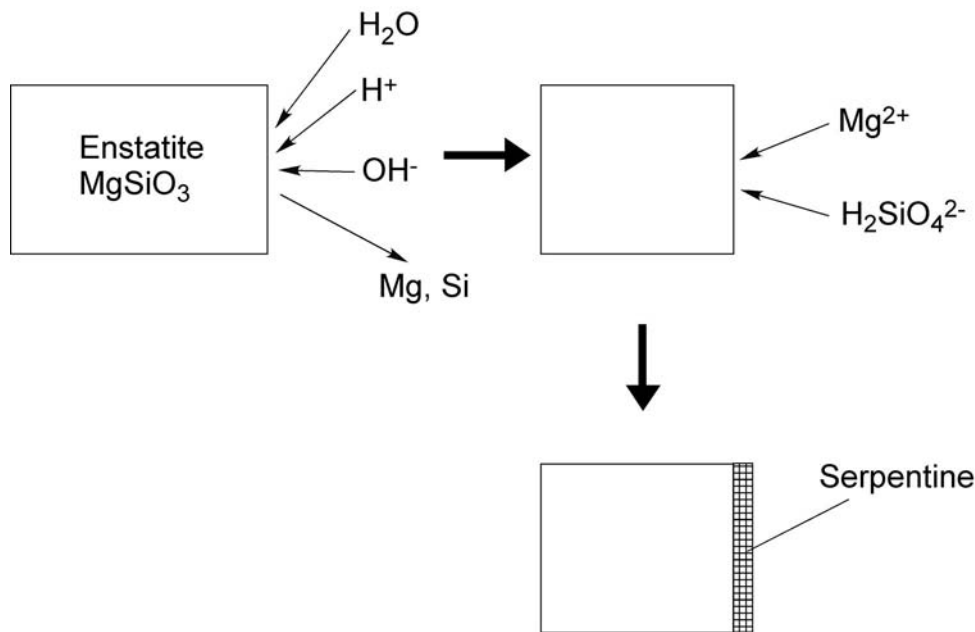


Figure 4.2: Proposed alteration process under neutral condition. Enstatite is dissolved by aqueous solution to release Mg and Si. Dissolved Mg and Si crystallize serpentine.

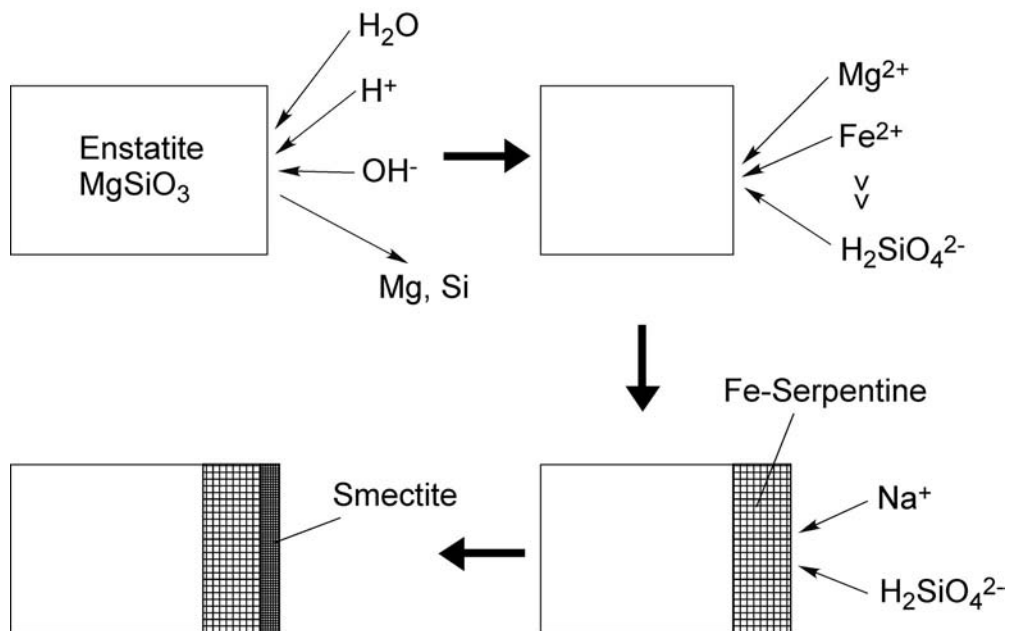
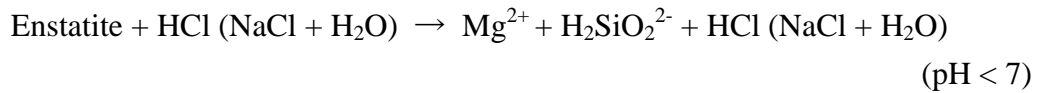


Figure 4.3: Proposed alteration process under Fe-rich and high pH solution. Enstatite is dissolved by alkaline solution to release Mg and Si. Much Mg, less Si, and Fe dissolved from Fe powder crystallize Fe-serpentine. Excess Si and Na in the residue solution crystallize smectite.

4.1.3 Acidic conditions

No change has been found from enstatite with 1N-HCl and 1N-NaCl solution (Fig. 3.1). These results suggest that no any phyllosilicates could form from enstatite under acidic conditions. Many dissolution experiments of enstatite (*e.g.*, Oelkers and Schott, 2001) indicated that enstatite more easily decomposes under acidic conditions compared with neutral and alkaline conditions. Enstatite treated with acid solutions in the present hydrothermal experiments may have decomposed, probably according to



Because phyllosilicates are unstable under acidic conditions, no the XRD peaks of new phase must appear. It is widely known that phyllosilicates such as serpentine also more easily decompose under acidic conditions compared with neutral and alkaline conditions (Bales and Morgan, 1985).

4.2 Comparison of hydrothermal experimental products with secondary minerals in aqueous altered chondrites

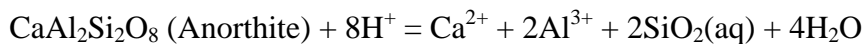
The present hydrothermal experiments of enstatite revealed that hydrous phyllosilicates could be easily produced by the reaction between enstatite and aqueous solution. It suggests that the secondary minerals replacing enstatite in chondrules of carbonaceous chondrites have been probably produced by the interaction between chondrules and aqueous fluid occurred in the chondritic parent body. And the difference of phyllosilicate mineralogy between chondrite clans regardless of the same precursor mineral was probably resulted from the difference of aqueous fluid. Here, I compare the secondary mineral assemblages obtained from hydrothermal experiments of enstatite with the assemblage of secondary mineral replacing enstatite in chondrules of carbonaceous chondrites to infer the difference of aqueous fluid between chondrite clans.

4.2.1 Comparison with enstatite in chondrules of CV chondrites

Based on TEM analysis, Keller and Buseck (1990) reported that Kaba CV chondrite has undergone pervasive aqueous alteration that resulted in the formation of Fe-bearing saponite in chondrules and matrix. They recognized that the saponite tends to have formed preferentially from enstatite in chondrules. In other some CV chondrites such as Mokoia (Tomeoka and Buseck, 1990; Kimura and Ikeda, 1998) and Bali (Keller and Buseck, 1994), enstatite in chondrules also tends to have been altered to saponite. Talc and biopyribole occur as replacing enstatite in Allende CV chondrite (Brearley, 1997), but these phyllosilicates are minor. So, smectite (saponite) is the dominant phyllosilicate replacing enstatite in chondrules of CV chondrites.

The smectite may have formed by the reaction between enstatite and Na-rich and high pH fluid such as was obtained from the runs with 0.1N- and 1N-NaOH solutions. Moreover, because serpentine, which occurs as an intergrowth with smectite, is a minor secondary hydrous phyllosilicate in chondrules of CV chondrites, the fluid must be poor in ferromagnesian ions such as Fe^{2+} . In chondrites, the candidates for the carrier phase of Na is mostly considered to be mesostasis glass that occurs in interstices between phenocrysts in chondrules and has similar composition to plagioclase (anorthite and albite). Alteration of the plagioclase-normative glass causes the

dissolution of Na and probably increases pH of the fluids due to leaching of Na and Ca according to



In fact, in chondrules of aqueously altered CV chondrites, most of mesostasis has been partially altered to hydrous phyllosilicates such as high-Al phyllosilicate and saponite (Tomeoka and Buseck, 1990; Keller and Buseck, 1990, 1994). Although ferromagnesian ions were probably supplied from Fe-Ni metal/sulfide and olivine in chondrules or matrix as discussed below, in CV chondrites, these phases must have been not or less affected by aqueous alteration (Krot et al., 1995). Therefore, in CV chondrites, partial alteration only of mesostasis glass must have occurred before or during alteration of enstatite.

4.2.2 Comparison with enstatite in chondrules of CM chondrites

CM chondrites have experienced higher degree of aqueous alteration and contained higher amounts of phyllosilicates in chondrules and matrix compared with CV chondrites (*e.g.*, McSween 1979). The only phyllosilicate in CM chondrites is essentially serpentine group mineral, including chrysotile, lizardite, antigorite and cronstedtite. Hanowski and Brearley (2001) have carried out systematic petrologic analyses of the aqueous alteration of various, well-defined textural chondrules in the ALH 81002 CM chondrites. They reported that enstatite in chondrules has been altered to ferroan Mg-serpentine at the earliest stage of aqueous alteration process. In other all CM chondrites such as Murray, Murchison, Mighei and LEW 90500 (*e.g.*, Hanowski and Brearley, 1997), enstatite tends to have been altered to serpentine with a variety of Mg/Fe ratio.

Based on the results of hydrothermal experiments of enstatite, there would be two possibilities for the fluid reacted with enstatite in CM chondrites: One has been Na-poor and relatively low pH, because smectite is minor hydrous phase. Another fluid reacted with enstatite in CM chondrites has been relatively Na-rich and high pH, but carried significant amounts of ferromagnesian ions such as Fe^{2+} .

Zolensky et al. (1989) simulated the reaction of anhydrous mineralogy using the EQ3/6 computer code to predict the evolving aqueous solution composition (Eh, pH, and species concentrations), amount and assemblage of alteration mineral that form. Calculated aqueous solution pH values vary from 7 to 12 for the alteration mineralogy of the CM chondrites. Tochilinite, which has the general formula $6\text{Fe}_{0.9}\text{S} \cdot 5((\text{Mg}, \text{Fe})(\text{OH})_2)$, widely occurs as a constituent mineral of poorly characterized phases

(PCP's) in chondrules and matrices of CM chondrites (*e.g.*, Tomeoka and Buseck, 1985). The hydrous phase is probably grew from aqueous solutions characterized by low fO_2 , high fS_2 , pH 10 to 12, and at a temperature at or below 170°C (Zolensky, 1984). Based on these results of both thermodynamic modeling and stability of hydrous minerals, the aqueous alteration of CM chondrites is considered to have occurred under high pH conditions. Thus, the fluid reacted with enstatite in CM chondrites must have been not only relatively Na-rich and high pH but also Fe-rich.

In chondrules of CM chondrites, rounded grains of Fe-Ni metal and sulfide have been widely altered to hydrous phases such as tochilinite, as well as mesostasis glass (Tomeoka and Buseck, 1985; Hanowski and Brearley, 2001; Chizmadia et al., 2002). Abundant serpentines occur in matrices of CM chondrites. The hydrous phyllosilicate probably has replaced fine-grained Mg-Fe-silicates such as Fe-rich olivine. The alteration of these Fe-rich phases in chondrules and matrix must have caused the increase of Fe^{2+} , as well as Mg^{2+} , Na^+ , Ca^{2+} , and $H_2SiO_4^{2-}$ in the fluid. Therefore, in CM chondrites, partial or complete alteration not only of mesostasis glass but also of Fe-Ni metal/sulfide and Fe-rich olivine must have occurred before or during alteration of enstatite.

4.3 Aqueous alteration scenarios of chondrites

Here, I propose the aqueous alteration scenarios of CV and CM chondrite clans, based on the results of the present experiments. Both chondrite clans differ about the assemblage of secondary mineral (*i.e.*, smectite or serpentine). I thought that the difference has been attributed to the primary mineral assemblages and then aqueous fluid involved in aqueous alteration.

4.3.1 Aqueous alteration scenario of CV chondrites

In the case of CV chondrites, the preferential alteration of the minerals having low resistance to the fluid must have proceeded. The resistance to aqueous alteration is considered to depend on the mineral chemistry (*e.g.*, Hanowski and Brearley, 2001). It is widely known that mesostasis glass in chondrules has been the weakest to aqueous alteration among constituent minerals in chondrites. Keller and Buseck (1990) recognized that chondrule glass is more susceptible to alteration than the fine-grained minerals in matrix and any other silicates in chondrules. Tomeoka and Kojima (1995) conducted hydrothermal experiments on Allende CV chondrite with 1N-HCl and they also recognized that the alteration proceeds much faster in chondrule mesostasis than in the fine-grained matrix. Thus, at the first stage of aqueous alteration in chondrites, the fluid must have preferentially attacked mesostasis glass in chondrules. And then, the alteration of these plagioclase-normative phases would have caused increase of alkali ion concentration and pH of the fluids.

The alkali-rich and high pH fluid became widespread in the bulk rock of chondrites, and in particular, permeated fractures and grain boundaries between constituent minerals. And then, in chondrules, enstatite phenocrysts have reacted with the fluid and been partially altered to smectite, due to the intrinsic fractures and twin lamellae as discussed below (see 4.4.1). Fe-Ni metal/sulfide grains and Mg-olivine phenocrysts have been probably less altered.

By the reaction with the alkali-rich and high pH fluid, Fe-rich olivine in matrix has been partially, *not completely*, altered to smectite (Tomeoka and Buseck, 1990; Keller and Buseck, 1990; Keller et al., 1994). Iishi and Han (1999) conducted hydrothermal experiments on Fe-rich olivine (Fa₅₀₋₁₀₀) with alkaline solutions at 50 to 200°C. They recognized that saponite was produced from Fa₅₀ with albite-rich solutions. And they suggested that the alteration of Bali CV chondrite was closely related to

aqueous solution that maintained high pH and carried significant dissolved solids such as Na, Al, and Si. Figure 4.4 shows a schematic model for aqueous alteration of CV chondrite discussed above.

4.3.2 Aqueous alteration scenario of CM chondrites

In the case of CM chondrites, at the same stage of the alteration of mesostasis glass, fine-grained Fe-rich olivine and Fe-Ni metal/sulfide in chondrules or matrix must have been partially or completely altered. By alteration of these Fe-rich phases, the fluid became enriched with ferromagnesian ions, although it was probably relatively Na-rich and high pH. In the case, serpentine became most stable among hydrous phase. Thus, in chondrules, enstatite phenocrysts reacted with the fluid to have been widely replaced by serpentine. The serpentine and tochilinite have also developed by replacing mesostasis glass and Fe-Ni metal/sulfide. As the alteration has progressed, Mg-rich olivine and any other silicates having relatively strong resistance to the fluids in chondrules would have been partially altered to serpentine. Figure 4.5 shows a schematic model for aqueous alteration of CM chondrite discussed above.

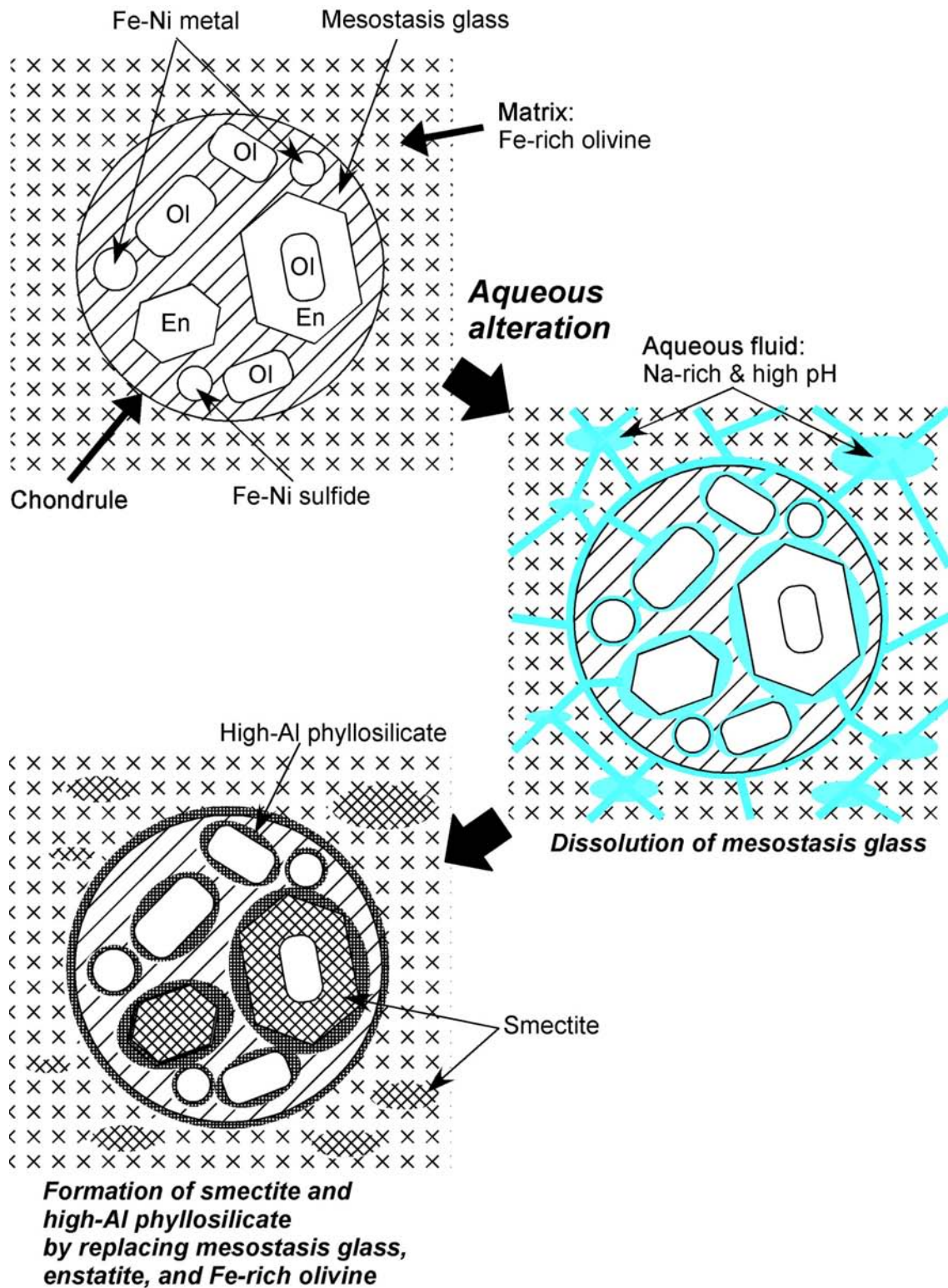


Figure 4.4: Model for aqueous alteration of CV chondrite. En: Enstatite, Ol: Olivine.

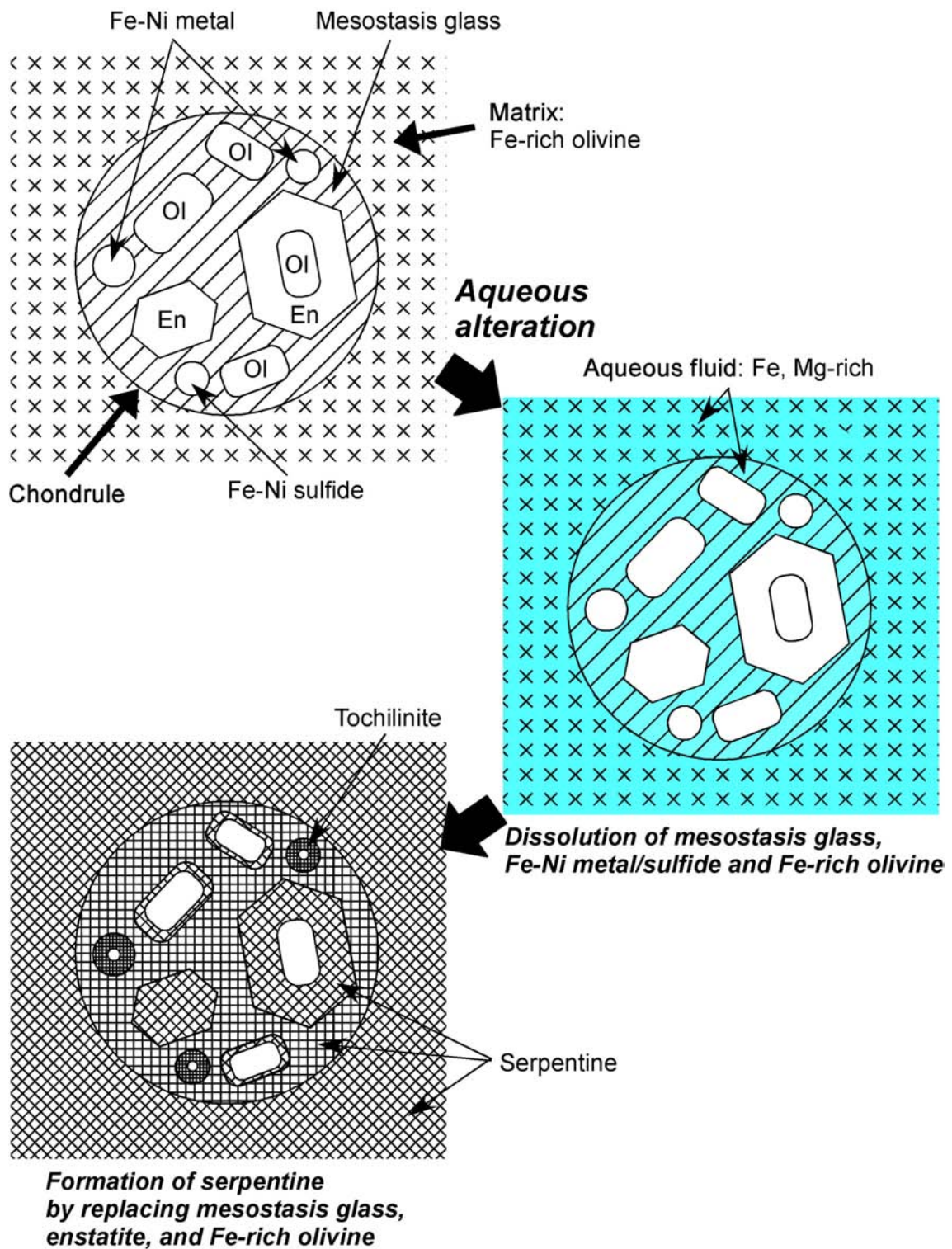


Figure 4.5: Model for aqueous alteration of CM chondrite. En: Enstatite, Ol: Olivine.

4.3.3 Initial water/rock ratio and pH of aqueous solution

As discussed above, the difference of the secondary minerals between CV and CM chondrites is probably attributed to the primary minerals involved in aqueous alteration. Why have the primary minerals involved in aqueous alteration differed between these chondrite clans? Although many factors have probably affected it, I here emphasize that two factors are important: initial water/rock ratio and pH of aqueous solution during aqueous alteration of chondrites.

If initial water/rock ratio were low, the content of dissolved ions in aqueous fluid would be low. In the case, the fluid would reach readily the saturation for the dissolved ions from altered phases and only the phase having less resistance such as mesostasis glass would dissolve to the fluid. As a result, the fluid would become Na^+ , Ca^{2+} , and $\text{H}_2\text{SiO}_4^{2-}$ -rich and high pH. If initial water/rock ratio were high, the content of dissolved ions in aqueous fluid would be high. In the case, the fluid would be hard to reach the saturation and most of constituent minerals, even the minerals having relatively strong resistance to the fluid such as olivine, would widely dissolve to the fluid. As a result, the fluid would become enriched with Fe^{2+} and Mg^{2+} . The former case would be for CV chondrites, the latter case would be for CM chondrites. The suggestion is strongly consistent with the contention by Nomura and Miyamoto (1998). They suggested that CV and CO chondrites have experienced aqueous alteration at low water/rock ratios, and CM chondrites have experienced high water/rock ratios, based on the hydrothermal experiments on refractory minerals such as gehlenite and spinel.

I cannot understand the initial pH value of the fluid, but can try to estimate the value by combination the suggestion discussed above with the mineral dissolution rate. It is widely known that most of silicates decompose more easily under acidic conditions compared with alkaline conditions (*e.g.*, Oelkers, 1999). Measured dissolution rate (moles/cm²/s) of olivine and albite glass at 25°C and pH~2 are approximately 10^{-12} and 10^{-16} , respectively, whereas those at 25°C and pH~12 are approximately 10^{-15} and 10^{-14} , respectively (Pokrovsky and Schott, 2000; Hamilton et al., 2001). As discussed above, I proposed that plagioclase-normative glass would mainly decompose in CV chondrites, and most of constituent minerals including glass and mafic silicates would decompose in CM chondrites. If it were corrected, in CM chondrites, the initial pH value of the fluid would be low to achieve the conditions that ferromagnesian ions would seem to dissolve abundantly in the fluid. On the other hands, in CV chondrites, the initial pH value of the fluid would be higher than that of CM chondrites to achieve the condition the preferential alteration of plagioclase-normative glass would occur.

4.4 Comparison of textures of hydrothermal altered enstatite with those of naturally altered enstatite in chondrites

The results of hydrothermal experiments on the mixtures of enstatite crystals and Fe with neutral and alkaline solutions (*Experiment 3*) provided the information about crystallographic features of alteration of enstatite and crystallographic relationships between enstatite and the secondary minerals. Here, I compare the textures of hydrothermally altered enstatite and naturally altered enstatite in chondrites.

4.4.1 Crystallographic features of enstatite alteration

From the present experiment (*Experiment 3*), clinoenstatite tends to be more strongly altered to serpentine compared with orthoenstatite under the same conditions. Clinoenstatite has been preferentially replaced by serpentine along fractures and twin lamellae in clinoenstatite crystals as well as along the margins of crystals (Figs. 3.11c-d and 3.12), whereas orthoenstatite has been replaced by serpentine along only the margins of crystals (Figs. 3.11a-b). It suggests that the low resistance of clinoenstatite to alteration has been obviously resulted from the occurrence of fractures and twin lamellae in a crystal. It is expected that abundant fractures and twin lamellae have increased the effective surface area of a crystal open to aqueous solution, and, as a result, promoted interaction between a crystal and aqueous solution. The fractures and twin lamellae have been formed by the inversion of protoenstatite to clinoenstatite during quenching of orthoenstatite heated at 1200°C (see 2.1).

In chondrites, clinoenstatite more abundantly occurs as phenocrysts of chondrules compared with orthoenstatite. It is widely known that clinoenstatite has been also formed by the inversion of protoenstatite to clinoenstatite during quenching of chondrule melts (*e.g.*, Brearley and Jones, 1998), like as the preparation of starting materials in the present experiment. Based on results of the present experiments, I suggest that enstatite (*i.e.*, clinoenstatite) has been *ab initio* more strongly affected by aqueous alteration compared with any other minerals in chondrules, due to intrinsic fractures and twin lamellae in an enstatite crystal (Fig. 4.6). In fact, at the earliest stage of aqueous alteration process, enstatite has been partially altered to phyllosilicate, whereas Ca-rich pyroxene and olivine, which occur as fresh grains containing no or less fractures and twin lamellae, have been not or less altered to phyllosilicates (*e.g.*,

Hanowski and Brearley, 2001).

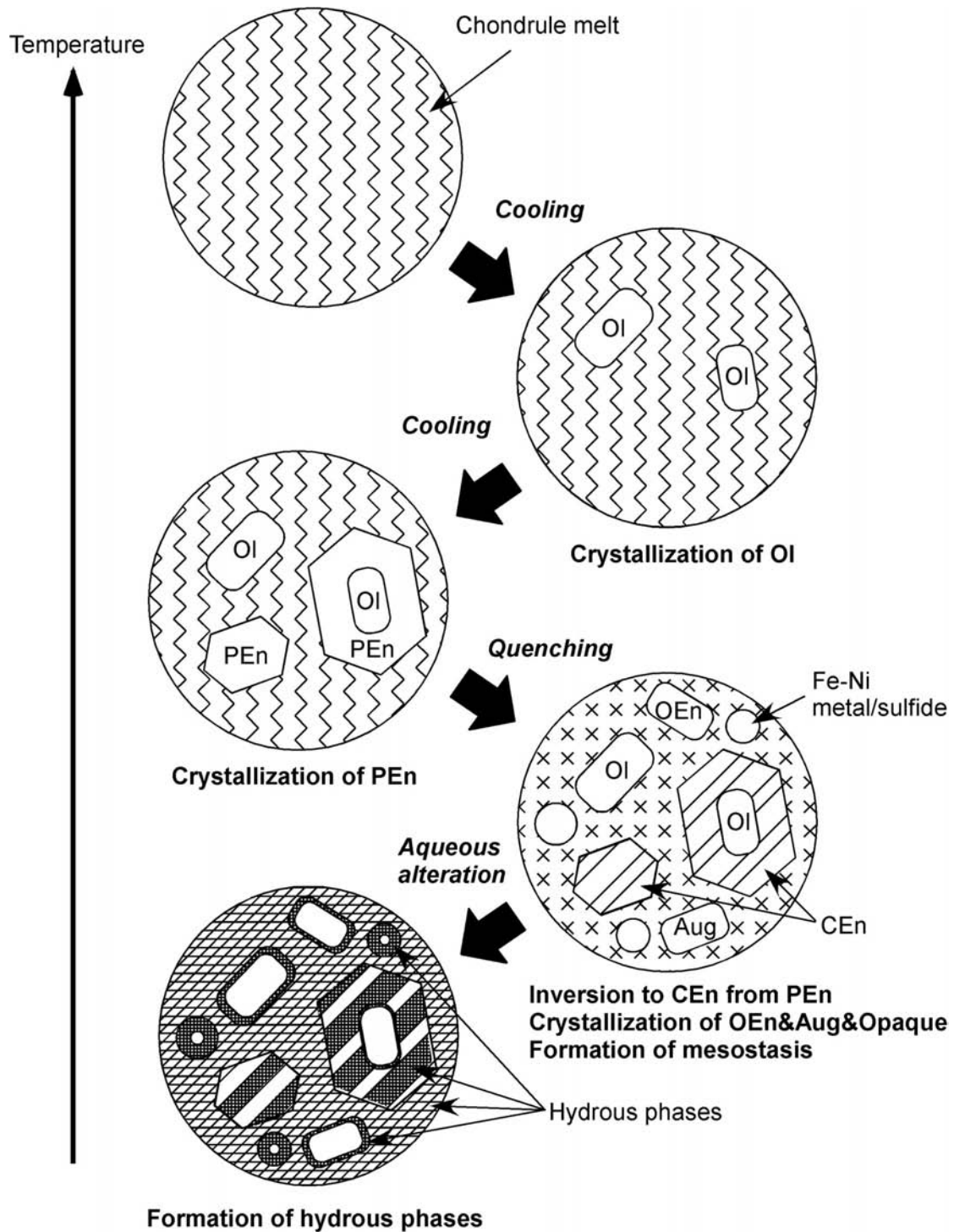


Figure 4.6: Model for formation mechanism and subsequent aqueous alteration process of chondrule containing a variety of silicate and opaque phases, including olivine (Ol), protoenstatite (PEn), clinoenstatite (CEn), orthoenstatite (OEn), augite (Aug), mesostasis, Fe-Ni metal/sulfide.

4.4.2 Crystallographic relationships between enstatite and the secondary minerals

In initiation of alteration of enstatite, the secondary mineral probably has particular crystallographic relation to enstatite such as Fe-poor topotactic serpentine in altered rims obtained from the mixtures of clinoenstatite and Fe with 1N-NaOH solution (Fig. 4.7). As the alteration proceeds, because availability of dissolved ions in aqueous solutions became increase, there is no particular crystallographic relationship between enstatite and the secondary mineral such as Fe-rich non-topotactic serpentine in veins (Fig. 4.7). From TEM observations of altered enstatite from terrestrial rocks (Le Gleuher et al., 1990), topotactic serpentine is a result of diffusion-controlled mechanism in restricted fluid flow, whereas random fine-grained serpentine is a result of a dissolution-neof ormation mechanism in highly fluid flux. It implies that the topotaxy of the secondary minerals replacing enstatite is probably indicator of the degree of aqueous alteration and the amount of aqueous fluid involved in the alteration.

Keller and Buseck (1990) reported that saponite replacing enstatite in chondrules of Kaba CV chondrite shows a crystallographic orientation relationship such that c^* of saponite parallels a^* of enstatite. Hanowski and Brearley (1997) reported that serpentine replacing chondrule silicates in LEW 90500 CM chondrite shows randomly oriented, fine-grained form. These features suggested that CM chondrites have experienced higher degree of aqueous alteration compared with CV chondrites, and then, the amount of aqueous fluid involved in the alteration would have been higher in CM chondrites compared with CV chondrites. It is strongly consistent with the contention by the results of the *Experiment 1* and *2* as discussed above.

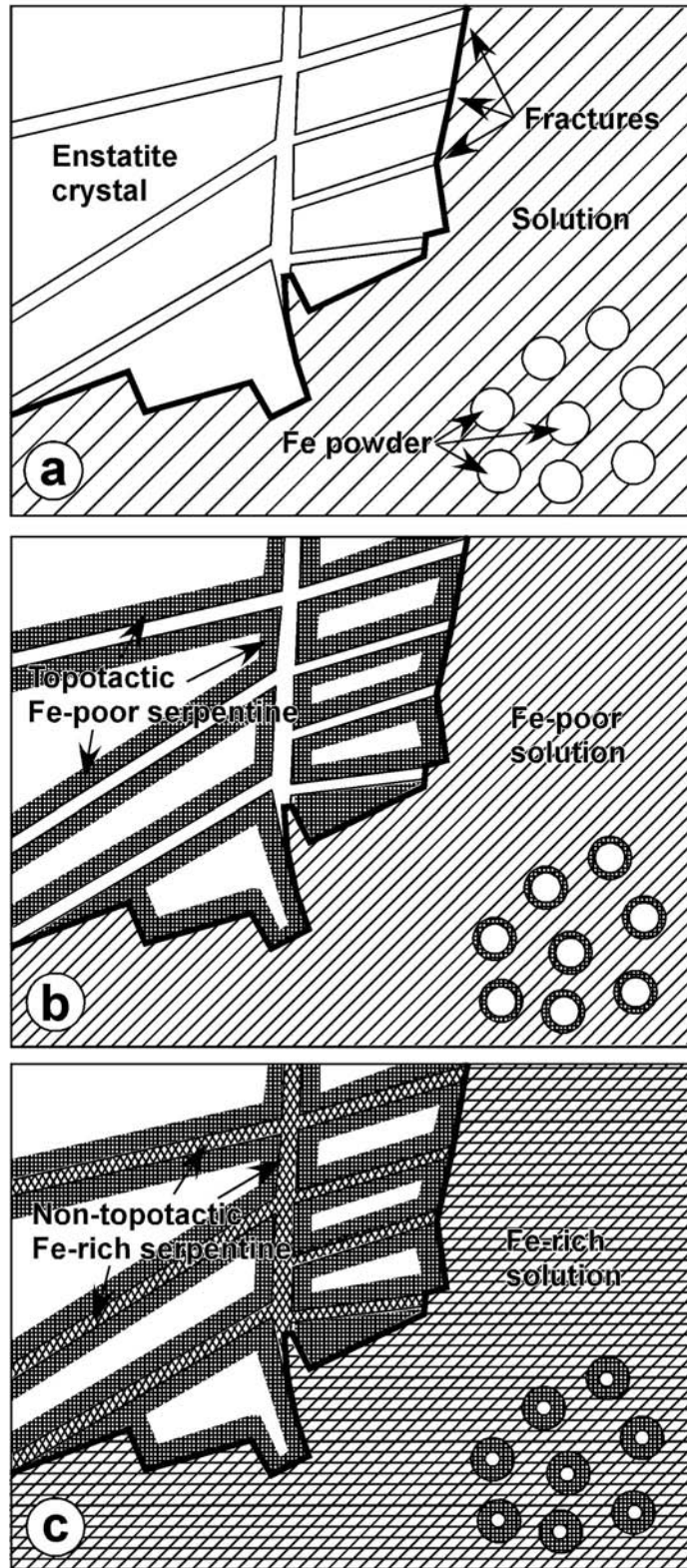


Figure 4.7: Schematic drawings for formation mechanism of the products by *Experiment 3*. Experimental time proceeds from (a) to (c). Note that solution probably became Fe-rich along with the experimental time, resulted from dissolution of Fe.

Conclusions for Part I

I carried out three series of hydrothermal experiments of enstatite.

The results of two experiments (*Experiment 1* and *2*) revealed that, under Na-rich alkaline conditions, smectite tends to be produced, whereas, under neutral to Na-poor weak alkaline conditions, serpentine tends to be produced. Simultaneously, smectite tends to be produced at higher temperature compared with serpentine. In addition, serpentine tends to be produced under Fe-rich alkaline conditions.

The results suggest that the secondary minerals replacing enstatite in chondrules of carbonaceous chondrites have been probably produced by the interaction between chondrules and aqueous fluid occurred in the chondritic parent body. And the difference of phyllosilicate mineralogy between chondrite clans regardless of the same precursor mineral was probably resulted from the difference of the aqueous fluid. Based on experimental results, I inferred that enstatite in chondrules of CV chondrites has probably reacted with Na-rich, Fe-poor and high pH aqueous solution, whereas that in chondrules of CM chondrites has probably reacted with Fe-rich and high pH aqueous solution.

Moreover, I hypothesized that difference of the aqueous fluid was probably derived from assemblage of the primary minerals involved in aqueous alteration. In CV chondrites, the preferential alteration only of mesostasis glass in chondrules has occurred before or during alteration of enstatite. On the other hands, in CM chondrites, alteration not only of mesostasis glass but also of Fe-Ni metal/sulfide and Fe-rich olivine in matrix or chondrules have occurred before or during alteration of enstatite. In addition, I inferred that the difference in the assemblage of the primary minerals involved in aqueous alteration has been probably resulted from initial water: rock ratio of aqueous alteration and initial pH value of aqueous fluid.

The results of another experiments (*Experiment 3*) revealed that there is a difference in degree of alteration between enstatite polymorph (*i.e.*, orthoenstatite and clinoenstatite). Clinoenstatite has been more strongly altered to hydrous phyllosilicates (serpentine) compared with orthoenstatite. Based on SEM and TEM studies of alteration textures of enstatites, I inferred that intrinsic fractures and twin lamellae in clinoenstatite are responsible for low resistance to alteration, and so, in chondrules, enstatite, which widely occurs as clinoenstatite rather than orthoenstatite, tends to be *ab*

initio more strongly affected by alteration compared with any other silicates. In addition, I reported that there is a difference in crystallographic relation to enstatite between serpentines produced by experiments (*i.e.*, topotactic and non-topotactic). Based on difference in texture between topotactic and non-topotactic serpentines, I suggested that topotactic serpentines have been formed by direct replacement of enstatite and non-topotactic serpentines have been formed by precipitation. Moreover, I proposed that topotaxy of phyllosilicates replacing precursor minerals indicates the degree of aqueous alteration in chondrites.

References for Part I

Bales R. C. and Morgan J. J. (1985) Dissolution kinetics of chrysotile at pH 7 to 10. *Geochim. Cosmochim. Acta* **49**, 2281-2288.

Brearley A. J. (1997) Disordered biopyriboles, amphibole, and talc in the Allende meteorite: Products of nebular or parent body aqueous alteration? *Science* **276**, 1103-1105.

Brearley A. J. and Duke C. L. (1998) Aqueous alteration of chondritic meteorites: Insights from experimental low temperature hydrothermal alteration of Allende (abstract). *Lunar Planet. Sci.* **XXIX** #1247.

Brearley A. J. and Jones R. H. (1998) Chondritic meteorites. In *Planetary Materials* (ed. J. J. Papike), Rev. Mineral., **36**. Mineralogical Society of America, Washington, USA.

Brearley A. J. and Jones C. L. (2002) Aqueous alteration of FeO-rich olivine: Insights from experimental alteration of Allende (abstract). **65th Annual Meteoritical Society Meeting** #5188.

Chizmadia L. J. and Brearley A. J. (2002) Petrographic study of chondrule mesostasis in the Yamato 791198 CM carbonaceous chondrite and comparison to ALH 81002 (abstract). *Lunar Planet. Sci.* **XXXIII** #2059.

Duke C. L. and Brearley A. J. (1998) Experimental aqueous alteration of Allende (CV3) (abstract). *Meteorit. Planet. Sci.* **33 (Suppl.)**, A43.

Duke C. L. and Brearley A. J. (1999) Experimental low temperature aqueous alteration of Allende under reducing conditions (abstract). *Lunar Planet. Sci.* **XXX** #1782.

Eggleton R. A. (1986) The relations between crystal structure and silicate weathering rates. In *Rates of chemical weathering of rocks and minerals* (eds. S. M. Colman and D.

P. Dethier), pp. 21-40. Academic Press, Orlando Florida.

Grimm R. E. and McSween H. Y. Jr. (1989) Water and the thermal evolution of carbonaceous chondrite parent bodies. *Icarus* **82**, 244-280.

Hamilton J. P., Brantley S. L., Pantano C. G., Criscenti L. J. and Kubicki J. D. (2001) Dissolution of nepheline, jadeite and albite glasses: Toward better models for aluminosilicate dissolution. *Geochim. Cosmochim. Acta* **65**, 3683-3702.

Hanowski N. P. and Brearley A. J. (1997) Transmission electron microscope observations of advanced silicate alteration in chondrules of the CM carbonaceous chondrite, Lewis Cliff 90500 (abstract). *Meteorit. Planet. Sci.* **32 (Suppl.)**, A56.

Hanowski N. P. and Brearley A. J. (2001) Aqueous alteration of chondrules in the CM carbonaceous chondrite, Allan Hills 81002: Implications for parent body alteration. *Geochim. Cosmochim. Acta* **65**, 495-518.

Iishi K. and Han X. J. (1999) Iron-rich olivine altered experimentally in alkaline solution: a study on aqueous alteration of Bali CV3 and Lance CO3 chondrites. *N. Jb. Miner. Mh.*

Iishi K., Torigoe K., and Han X. J. (1997) Oriented precipitate complexes in iron-rich olivines produced experimentally in aqueous oxidizing environment. *Phys. Chem. Minerals* **25**, 8-14.

Jones R. H. (1994) Petrology of FeO-poor, porphyritic pyroxene chondrules in the Semarkona chondrite. *Geochim. Cosmochim. Acta* **58**, 5325-5340.

Jones C. L. and Brearley A. J. (2000) Transmission electron microscope observations of phyllosilicate development during experimental aqueous alteration of Allende (abstract). *Lunar Planet. Sci.* **XXXI** #1204.

Keller L. P. and Buseck P. R. (1990) Aqueous alteration in the Kaba CV3 carbonaceous chondrite. *Geochim. Cosmochim. Acta* **54**, 2113-2120.

Keller L. P., Thomas K. L., Clayton R. N., Mayeda T. K., DeHart J. M. and McKay D. S.

(1994) Aqueous alteration of the Bali CV3 chondrite: Evidence from mineralogy, mineral chemistry, and oxygen isotopic compositions. *Geochim. Cosmochim. Acta* **58**, 5589-5598.

Kimura M. and Ikeda Y. (1998) Hydrous and anhydrous alterations of chondrules in Kaba and Mokoia CV chondrites. *Meteorit. Planet. Sci.* **33**, 1139-1146.

Kojima T. and Tomeoka K. (1999) Experimental hydrothermal alteration of the Allende CV3 chondrite under acidic and neutral conditions (abstract). *Meteorit. Planet. Sci.* **34** (Suppl.), A67.

Kojima T. and Tomeoka K. (2000) Transmission electron microscopy of phyllosilicates in experimentally altered Allende: Comparison to naturally altered CV3 chondrites (abstract). *Meteorit. Planet. Sci.* **35** (Suppl.), A90.

Krot A. N., Scott E. R. D. and Zolensky M. E. (1995) Mineralogical and chemical modification of components in CV3 chondrites: Nebular or asteroidal processing? *Meteoritics* **30**, 748-775.

Le Gleuher M., Livi K. J. T., Veblen D. R., Noack Y., and Amouric M. (1990) Serpentinization of enstatite from Pernes, France: Reaction microstructures and the role of system openness. *Am. Mineral.* **75**, 813-824.

McSween H. Y. Jr. (1979) Are carbonaceous chondrites primitive or processed? A review. *Rev. Geophys. Space Phys.* **17**, 1059-1078.

Moroz L. V., Kozerenko S. V., and Fadeev V. V. (1997) The reflectance spectrum of synthetic tochilinite (abstract). *Lunar Planet. Sci.* **XXVIII** #1288.

Nomura K. and Miyamoto M. (1998) Hydrothermal experiments on alteration of Ca-Al-rich inclusions (CAIs) in carbonaceous chondrites: Implication for aqueous alteration in parent asteroids. *Geochim. Cosmochim. Acta* **62**, 3575-3588.

Oelkers E. H. (1999) A comparison of enstatite and forsterite dissolution rates and mechanisms. In *Growth and Dissolution in Geosystems* (eds. B. Jamveit and P. Meakin) pp. 253-257, Kluwer.

Oelkers E. H. and Schott J. (2001) An experimental study of enstatite dissolution rates as a function of pH, temperature, and aqueous Mg and Si concentration, and the mechanism of pyroxene/pyroxenoid dissolution. *Geochim. Cosmochim. Acta* **65**, 1219-1231.

Ozima M. (1982) Growth of orthoenstatite crystals by the flux method. *J. Jpn. Assoc. Mineral. Petrol. Econ. Geol. (Suppl.)*, **3**, 97-103 (in Japanese).

Pokrovsky O. S. and Schott J. (2000) Kinetics and mechanism of forsterite dissolution at 25°C and pH from 1 to 12. *Geochim. Cosmochim. Acta* **64**, 3313-3325.

Sato K, Miyamoto M., and Mikouchi T. (2002) Hydrothermal experiments on several chondrites at low temperatures: pH change of solution (abstract). **65th Annual Meteoritical Society Meeting** #5133.

Stumm W. and Morgan J. J. (1996) *Aquatic Chemistry: Chemical equilibria and rates in natural water*, Third edition. Wiley-Interscience, 1022p.

Takatori K., Tomeoka K., Tsukimura K. and Takeda H. (1993) Hydrothermal alteration experiments of olivine with varying Fe contents: An attempt to simulate aqueous alteration of the carbonaceous chondrites (abstract). *Lunar Planet. Sci.* **XXIV** #1389.

Tomeoka K. and Buseck P. R. (1985) Indicators of aqueous alteration in CM carbonaceous chondrites: Microtextures of a layered mineral containing Fe, S, O and Ni. *Geochim. Cosmochim. Acta* **49**, 2149-2163.

Tomeoka K. and Buseck P. R. (1990) Phyllosilicates in the Mokoia CV carbonaceous chondrite: Evidence for aqueous alteration in an oxidizing condition. *Geochim. Cosmochim. Acta* **54**, 1745-1754.

Tomeoka K. and Kojima T. (1995) Experimental aqueous alteration of the Allende CV3 chondrite (abstract). *Meteoritics* **30**, 588-589.

Zolensky M. E. (1984) Hydrothermal alteration of CM carbonaceous chondrites: Implications of the identification of tochilinite as one type of meteoritic PCP (abstract).

Meteoritics **19**, 346-347.

Zolensky M. E. and McSween H. Y. Jr. (1988) Aqueous alteration. In *Meteorites and the Early Solar System* (eds. J.F. Kerridge and M.S. Matthews), pp. 114-143. Univ. Arizona, Tucson, Arizona.

Zolensky M. E., Bourcier W., and Gooding J. L. (1989) Aqueous alteration on the hydrous asteroids: Results of EQ3/6 computer simulations. *Icarus* **78**, 411-425.

Part II

Modeling aqueous alteration of chondrules: Results of the Geochemist's workbench

Chapter 5

General Introduction

5.1 Previous modeling studies of aqueous alteration of the carbonaceous chondrites using computer code

The carbonaceous chondrites contain a variety of hydrous phases. It has been widely considered that aqueous alteration has occurred on their parent body (or bodies). In order to understand physico-chemical conditions of the alteration, a variety of studies, including petrographic study, isotopic study, and hydrothermal experimental study (see Part I), have been performed by many workers. Modeling study using computer code is one of them. Zolensky et al. (1989) and Bourcier and Zolensky (1991, 1992) examined aqueous alteration scenarios for CM and CV asteroidal parent bodies for a wide range of temperature and water-rock ratios, using the EQ3/R computer code (Wolery, 1992) or the REACT computer code (Bethke, 1996). Rosenberg et al. (2001a, b) examined an inorganic geochemical modeling study of the aqueous alteration of CM asteroidal parent bodies for the oxidized-Fe and the reduced-Fe endmember precursor assemblages. Aqueous alteration of the Martian surface has been also modeled with a chemical equilibrium computer code (Bourcier et al., 1988; Wallendahl and Treiman, 1999).

5.2 Aqueous alteration of chondrules

Chondrules are the most abundant components of chondrites, comprising <80% of ordinary and enstatite chondrites and >15% of carbonaceous chondrites except for CI clan, which lacks chondrules. They are sub-millimeter-sized igneous spherules composed mainly of ferromagnesian silicates (olivine, pyroxene, and a feldspathic glass). Chondrules are considered to have formed in the early solar nebula and accreted into the chondritic parent bodies, as well as matrix particles and refractory inclusions (Brearley and Jones, 1998).

Aqueous alteration has modified chondrule mineral compositions and textures

in various degrees. Because chondrules originally contain a wide variety of minerals, the alteration mineral assemblages and textures shows complex and chaotic. For instance, altered chondrules contain hydroxide, oxide, sulfide, hydrous phyllosilicates, including serpentine group (antigorite, chrysotile, cronstedtite), smectite group, chlorite group, mica, and talc. Clarification of the formation process of these phases and mechanism of aqueous alteration of chondrules would provide information about physic-chemical conditions for aqueous alteration on the parent body (or bodies) (*e.g.*, water/rock ratio, temperature, pH and Eh of aqueous fluids).

5.3 The purposes of modeling of aqueous alteration of chondrules

Previous modeling aqueous alteration studies of chondrites have focused alteration on bulk rocks in order to explore asteroidal alteration conditions. However, chondrites have experienced unequilibrated alteration. In the case, it is important to understand the mechanism of alteration of each component (*e.g.*, chondrule, matrix, refractory inclusions) or each constituent mineral (*e.g.*, olivine, pyroxene etc.). I modeled aqueous alteration of chondrules and predicted the alteration mineral assemblages, using the computer code. Then, I compared the predicted alteration mineral assemblages with natural alteration mineral assemblages. I here present the preliminary results. The purpose of this study is to infer how chondrules having a multi-component system have been modified by interaction with aqueous fluids.

Chapter 6

Computer Simulations

6.1 Scenarios of aqueous alteration of chondrules

I assumed three models for aqueous alteration of chondrules as follows.

Model 1: Equilibrated aqueous alteration. Precursor minerals in chondrule are completely altered to hydrous phases.

Model 2: Unequilibrated aqueous alteration. Enstatite, mesostasis and Fe-Ni metal and sulfide between precursor minerals in chondrule are completely altered to hydrous phases.

Model 3: Unequilibrated aqueous alteration. Enstatite and mesostasis are partially altered to hydrous phases.

I will describe detail about these models further below.

6.1.1 Model 1

Model 1 is assumed that chondrule reacted with significant amount of aqueous solution to reach the equilibrium (Fig. 6.1). The system in the model contains all precursor minerals in chondrule.

In chondrites, chondrules show a wide variety of textures, including porphyritic olivine (PO), porphyritic olivine-pyroxene (POP), porphyritic pyroxene (PP), barred olivine (BO), radial pyroxene (RP). Although these chondrule types consist mainly of olivine, pyroxene, a feldspathic glass, Fe-Ni metal and sulfide, etc, the proportion of these constitute minerals differ between chondrule types. Porphyritic chondrules constitute >90% of all chondrules in the carbonaceous chondrites (Grossman et al., 1988). I selected POP and PO as unaltered precursor chondrule types.

It is difficult to determine the original, unaltered mineral compositions of POP and PO chondrules, because mineralogy of chondrules of the carbonaceous chondrites has not been a little modified by alteration. I reply on the Browning and Bourcier (1998) study that examined possible precursor mineralogy of the CM carbonaceous chondrites

by mass balance analyses. They estimated of original phase proportions of PO and POP chondrules, using data from Rubin and Wasson (1986). The estimated POP chondrule consists of pyrrhotite (0.14 vol%), glass (2.37), forsterite (48.71), enstatite (48.39), chromite (0.07) and kamacite (0.32). The estimated PO chondrule consists of pyrrhotite (0.07 vol%), glass (4.37), forsterite (95.36), enstatite (0.00), chromite (0.00) and kamacite (0.20). The estimation has been conducted by using unaltered chondrule average bulk compositions, and so I adopted the estimated phase proportion as the original, unaltered mineral compositions of POP and PO chondrules in the model. I simplified kamacite to Fe. In addition, I slightly modified their estimated phase proportions of POP and PO chondrules, because they have regarded mesostasis as SiO₂-rich glass. Many petrographic studies (*e.g.*, Jones 1994) reported that unaltered mesostasis in chondrules has similar composition to mixing of plagioclase (anorthite and albite) and Ca-rich pyroxene (diopside). I substituted SiO₂-rich glass to plagioclase and Ca-rich pyroxene as mesostasis in phase proportion. Precursor mineralogy and the phase proportion are listed in Table 6.1.

6.1.2 Model 2

It is widely known that there is a difference in resistance to aqueous alteration between constituent minerals in chondrule (see Part I). Enstatite, mesostasis and Fe-Ni metal and sulfide tends to be more strongly affected by alteration compared with any other phases in chondrules. In order to investigate aqueous alteration of these phases, I assumed *Model 2* (Fig. 6.2a), in which the system contained enstatite, mesostasis and Fe-Ni metal and sulfide. The phase proportion of these phases was similar to that of POP chondrule in *Model 1*. It is listed in Table 6.1.

6.1.3 Model 3

I was further interested in minor degree of aqueous alteration. I assumed *Model 3* (Fig. 6.2b), in which the system contains only enstatite and mesostasis. The phase proportion of enstatite and mesostasis in the model differs from that of POP chondrule in *Model 1*. In the case of *Model 1*, enstatite/mesostasis volume ratio is about 23, whereas, in the case of *Model 3*, the ratio is about 2.3, assuming that mesostasis is more strongly altered compared with enstatite. The phase proportion is listed in Table 6.1.

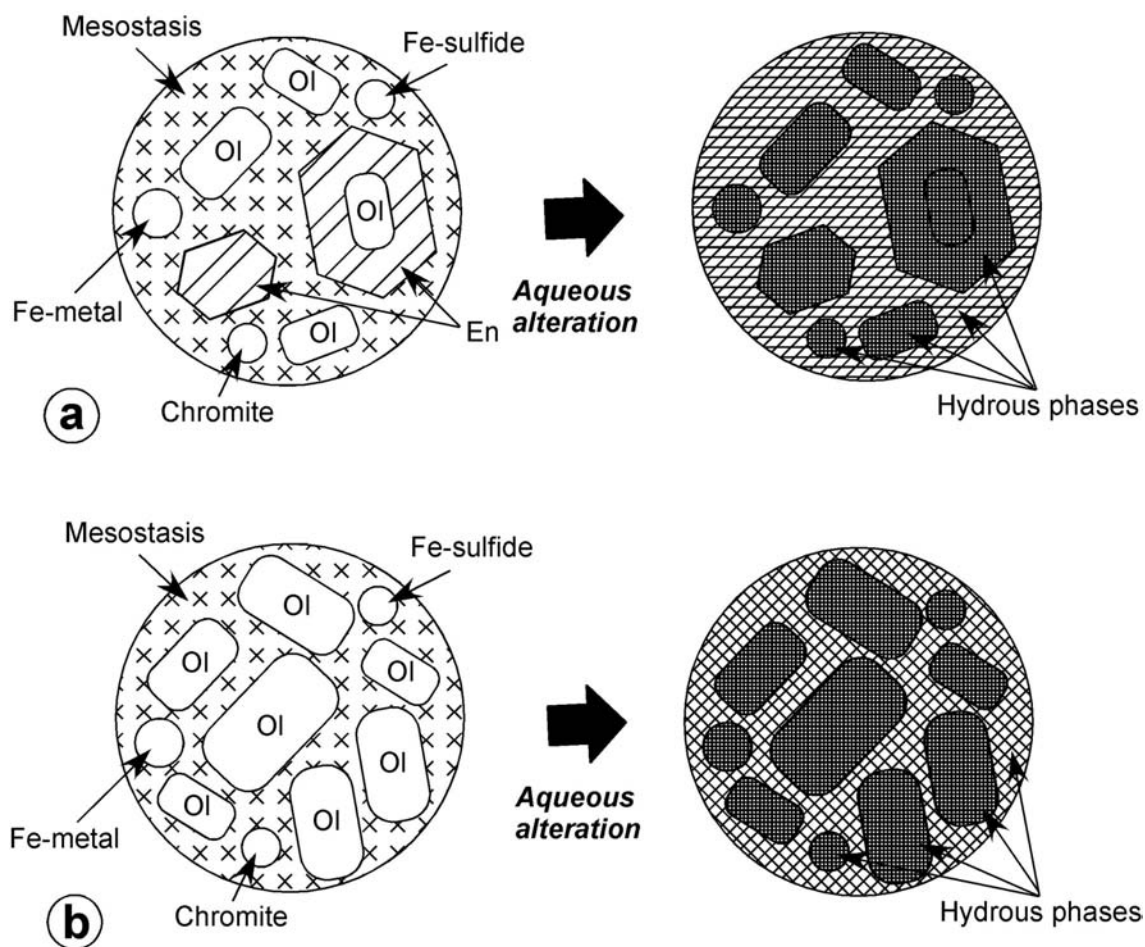


Figure 6.1: Schematic drawings of possible equilibrated aqueous alteration of POP (a) and PO (b) chondrules, based on *Model 1*. Ol = olivine, En = enstatite.

Table 6.1: Precursor mineralogy and mineral fomulae

Mineral name	Mineral fomula	Porportion (wt%)			
		Model 1 ^a		Model 2	Model 3
		POP	PO		
Pyrrhotite	$\text{Fe}_{0.875}\text{S}$	0.22	0.1	0.42	0
Anorthite	$\text{CaAl}_2\text{Si}_2\text{O}_8$	0.81	1.5	1.58	11.8
Albite	$\text{NaAlSi}_3\text{O}_8$	0.77	1.42	1.52	11.2
Diopside	$\text{CaMgSi}_2\text{O}_6$	0.49	0.89	0.94	7
Forsterite	Mg_2SiO_4	48.6	95.6	0	0
Enstatite	$\text{Mg}_2\text{Si}_2\text{O}_6$	48.2	0	94	70
Chromite	FeCr_2O_4	0.12	0	0	0
Native iron metal	Fe	0.79	0.49	1.54	0
		100	100	100	100

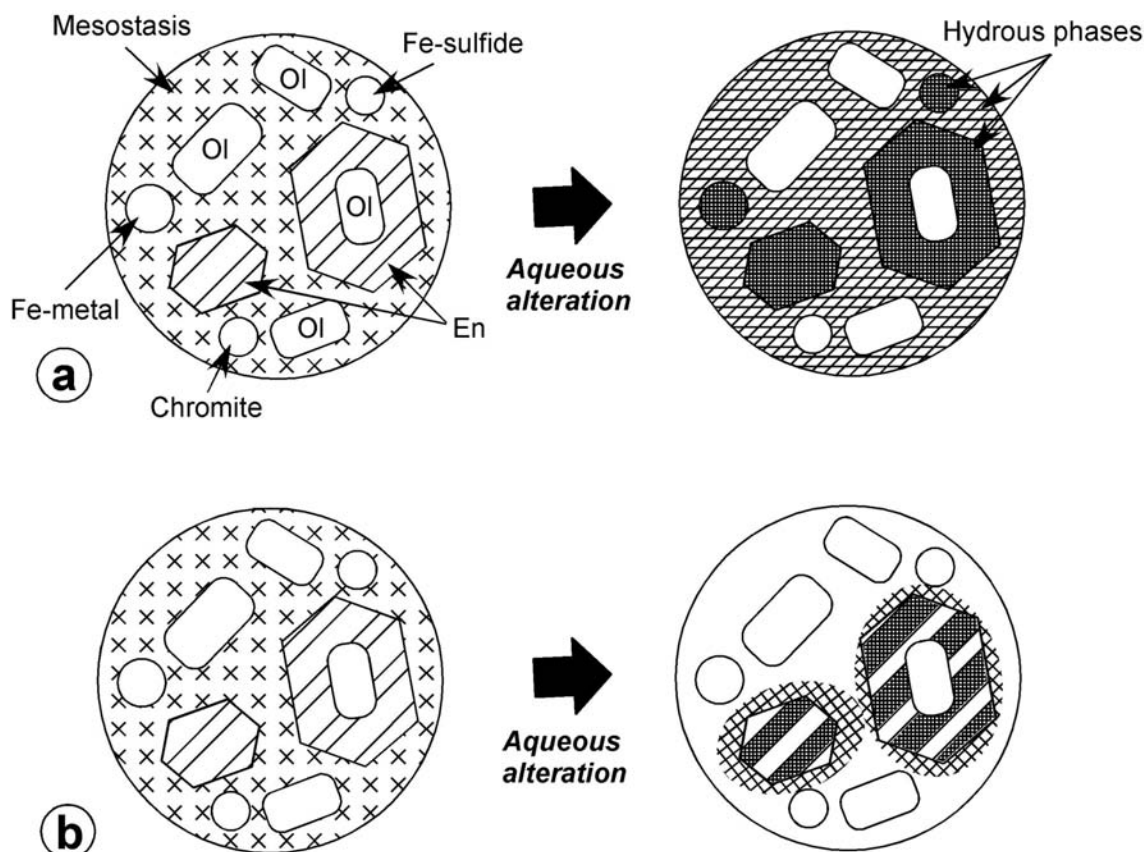


Figure 6.2: Schematic drawings of possible unequilibrated aqueous alteration of POP chondrule. (a) Enstatite, mesostasis, and Fe-Ni metal and sulfide have been altered to hydrous phases (*Model 2*), (c) Enstatite and mesostasis have been partially altered to hydrous phases (*Model 3*). Ol = olivine, En = enstatite.

6.2 Modeling study

I run simulations of three models, described in the previous section, to explore behavior of aqueous alteration of chondrules. My calculations are performed using the REACT computer code (Bethke, 1996). REACT is a geochemical modeling tool comprised in the Geochemist's Workbench[®] (GWB) that is a set of interactive software tools for solving problems in aqueous geochemistry. The program is similar to the EQ3/6 code (Wolery, 1992), which is more commonly used (*e.g.*, Zolensky et al., 1989).

REACT models equilibrium states and geochemical processes in systems that contain an aqueous fluid, with or without mineral phases in it. The program can calculate the equilibrium distribution of aqueous species, fluid saturation state with respect to minerals, and the fugacities of dissolved gases. REACT traces the evolution of the system in response to changes in temperature or the addition or removal of

reactants and calculate the equilibrium mineral assemblages. The program also can integrate kinetic rate law.

REACT works by using a thermodynamic database. The database contains the properties of aqueous species, minerals, gases, and equilibrium constants for reactions to form these species. The most commonly used dataset is “thermo.dat” based in large part on the SUPCRT92 data compilation (Johnson et al., 1992). However, the dataset does not contain thermodynamic data for cronstedtite, greenalite, and tochilinite, which occurs as alteration products in the CM carbonaceous chondrites. My calculation adopted “thermo. com. V8. R6+. dat” as thermodynamic dataset. This is the Lawrence Livermore National Laboratories (LLNL) version 8, release 6 “combined” dataset containing thermodynamic data for cronstedtite and greenalite. In addition, thermodynamic dataset for Fe-endmember tochilinite were estimated by assuming ideal mixing pyrrhotite and iron hydroxide layers (Browning and Bourcier, 1996).

Each calculation begins with addition of unaltered chondrule which has phase proportion assumed in each model to significant amount of NaCl electrolyte solution. The fluid must be NaCl electrolyte solution rather than dilute H₂O in view of resolving charge balance in a fluid. Initial pH value of NaCl electrolyte solution was 7. I do not know the original proportions of chondrule and water reacted with it in chondrites. Because most of hydrous phases need significant amount of aqueous solution to supersaturate in a fluid, the proportion of chondrule and NaCl electrolyte solution was assumed to range in weight ratio from 0.32 to 0.022 in each model. I also do not know alteration temperature in chondrites. Because most of hydrous phases are stable at lower temperature rather than higher temperature, temperature was set to room temperature (25°C) in all calculation. In addition, I do not know oxygen fugacity on alteration of chondrites. In all calculation, oxygen fugacity was set to 0.2 bars for convenience. After each calculation, the equilibrium mineral assemblage was calculated. I examined the mineral assemblages, changes in pH and Eh values of aqueous solution and concentration of dissolved ions in each model to explore the effect of aqueous alteration of chondrules.

Chapter 7

Results and Discussion

7.1 Comparison of the predicted mineral assemblage from GWB with alteration mineral assemblage in chondrules

Table. 7.1 shows alteration phases predicted from REACT in all model. The alteration phases have abundant variety of mineral group, including serpentine, smectite, chlorite, talc, zeolite, garnet, hydroxide, and oxide. At each calculation, the precipitations of mineral phases well known to be kinetically inhibited at low temperatures (*e.g.*, amphiboles) were suppressed. The alteration mineral assemblage differs between three models. Each result in detail is described as follows.

Table 7.1: Alteration phases and mineral formulae.

Mineral name	Mineral formula	Mineral group
Andradite	$\text{Ca}_3\text{Fe}_2(\text{SiO}_4)_3$	Garnet
Antigorite	$\text{Mg}_{48}\text{Si}_{24}\text{O}_{85}(\text{OH})_{62}$	Serpentine
Brucite	$\text{Mg}(\text{OH})_2$	Hydroxide
Clinochlore-14A	$\text{Mg}_5\text{Al}_2\text{Si}_3\text{O}_{10}(\text{OH})_8$	Chlorite
Daphnite-14A	$\text{Fe}_5\text{AlAlSi}_3\text{O}_{10}(\text{OH})_8$	Chlorite
Diaspore	AlHO_2	Hydroxide
Greenalite	$\text{Fe}_3\text{Si}_2\text{O}_5(\text{OH})_4$	Serpentine
Hematite	Fe_2O_3	Oxide
Magnetite	Fe_3O_4	Oxide
Mesolite	$\text{Na}_{0.676}\text{Ca}_{0.657}\text{Al}_{1.99}\text{Si}_{3.01}\text{O}_{10} \cdot 2.647\text{H}_2\text{O}$	Zeolite
Ripidolite-14A	$\text{Mg}_3\text{Fe}_2\text{Al}_2\text{Si}_3\text{O}_{10}(\text{OH})_8$	Chlorite
Saponite-Na	$\text{Na}_{0.33}\text{Mg}_3\text{Al}_{0.33}\text{Si}_{3.67}\text{O}_{10}(\text{OH})_2$	Smectite
Talc	$\text{Mg}_3\text{Si}_4\text{O}_{10}(\text{OH})_2$	Talc
Tochilinite	$6\text{FeS} \cdot 5\text{Fe}(\text{OH})_2$	Tochilinite

7.1.1 Model 1

In *Model 1*, 1 kg of aqueous solution reacts 320 g of minerals that is equivalent to 100 cm³ of chondrule. Fig. 7.1 and Fig. 7.2 show calculation results from *Model 1*.

In both POP and PO chondrules, the predicted predominant product is serpentine (antigorite), followed by brucite, chlorite group (clinochlore-14A, daphnite-14A, and ripidolite-14A), zeolite (mesolite), tochilinite, andradite, and magnetite. In the case of POP chondrule (Fig. 7.1), smectite group (saponite-Na) occurred in the earliest stage of aqueous alteration, but the abundance gradually decreased with alteration progress, suggesting the phase is metastable in the system. These results suggest that, if POP and PO chondrules have been completely altered, chondrule pseudomorphs after aqueous alteration would be composed predominantly of serpentine. The suggestion is consistent with the petrographic study of the CM1 carbonaceous chondrites (e.g., EET83334, ALH88045, and clasts in Kaidum meteorite) (Zolensky et al., 1997). The chondrite clan has experienced extensive aqueous alteration and contains phyllosilicate-dominated aggregates that are obviously relict chondrules or chondrule pseudomorphs after aqueous alteration. The aggregates consist mainly of serpentine (probably antigorite) with Fe-Ni sulfide and minor clinochlore. And tochilinite has not been reported in the chondrite clan (Zolensky et al., 1997). In the model, tochilinite is a minor phase (Fig. 7.1). It is also a consistent result between the petrographic study and computer simulation.

In the case of POP, the pH increases from 10.25 to about 11.5 and Eh decreases from -0.5 to about -0.7 (Fig. 7.1). And, in the case of PO, the pH increases from 10.75 to about 12.25 and Eh decreases from -0.4 to about -0.8 along with alteration progress (Fig. 7.2). These results for both cases suggest that complete alteration of chondrule causes alkaline and reducing condition. Dominated ion in aqueous solution is Ca²⁺, followed by Al³⁺, SiO₂ (aq) (*i.e.*, H₄SiO₄⁻). These ion concentrations gradually increased along with alteration progress. They were obviously derived from dissolution of mesostasis phases. On the other hands, Mg²⁺ ion concentrations gradually decreased, and so aqueous solution became be depleted in Mg²⁺. The ion was probably consumed the formation of serpentine. Sato et al. (2002) conducted hydrothermal experiments of several chondrites, including Allende (CV), Murchison (CM), and Nuevo Mercurio (H5), at low temperatures (50-200°C) and analyzed ion concentrations of aqueous solution after experiments by using ICP-AES. They reported that the amount of Ca, as well as Na and S, dissolved in aqueous solution are high relative to the bulk composition of each meteorite, and suggested that these ions are highly soluble. It is consistent with the result of the computer simulations for the case of Ca ion. And I

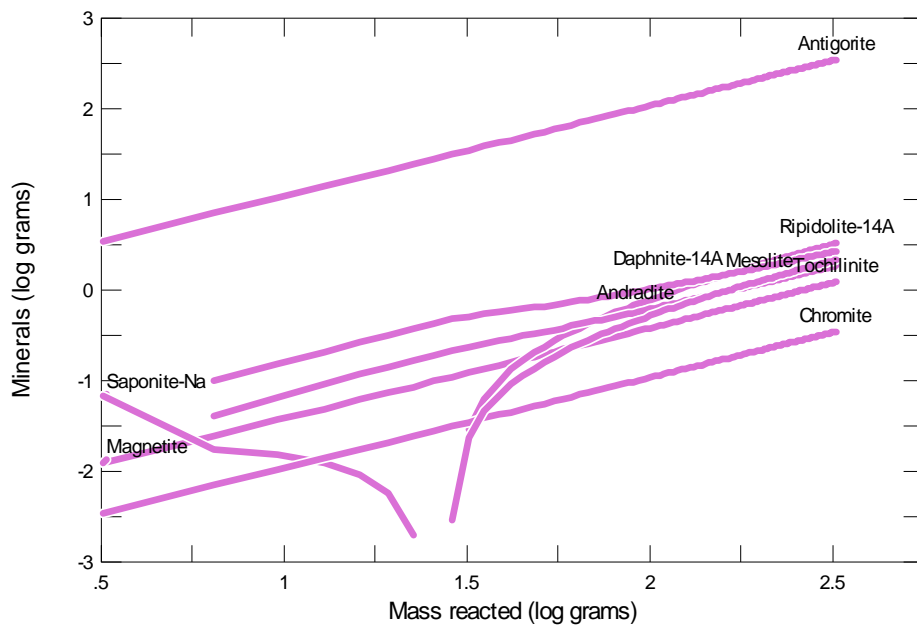
suggest that mesostasis in chondrule is major source of Ca to aqueous solution during alteration.

7.1.2. Model 2

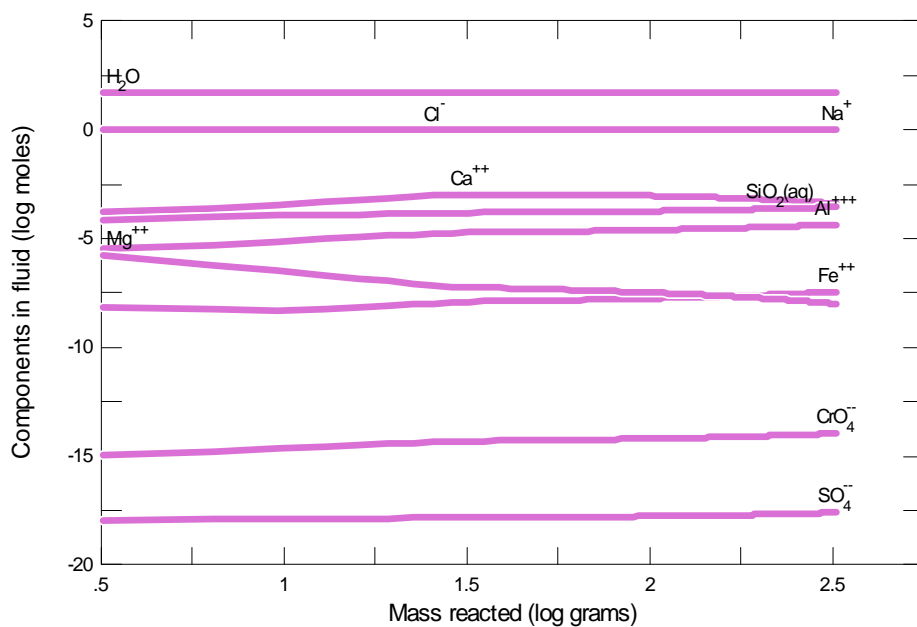
Fig. 7.3 shows calculation result from *Model 2*. Serpentine group (antigorite and greenalite) is dominant phase. Minor phases are talc, smectite (saponite-Na), and tochilinite. Except for talc, these phases have been recognized in chondrules of lightly to moderately altered CM carbonaceous chondrites (*e.g.*, Murchison, Mighei, Bells). Compared to *Model 1*, Fe-rich serpentine (greenalite) is predicted to form. This result suggests that unequilibrated aqueous alteration of chondrule tends to produce Fe-rich serpentine compared with equilibrated aqueous alteration. Systematic petrographic studies (*e.g.*, McSween, 1979; Tomeoka and Buseck, 1985; Hanowski and Brearley, 2001) suggests that Fe-rich serpentine (*e.g.*, cronstedtite) tends to be produced at the earliest stage of aqueous alteration in chondrules of CM chondrites and Fe/(Fe+Mg) ratio of produced serpentine has decreased along with alteration progress. So, the petrographic result is consistent with the result of the model.

7.1.3. Model 3

Fig. 7.4 shows calculation result from *Model 3*. Smectite (saponite-Na) is dominant phase. Serpentine (antigorite), mesolite and diopside are also present. Except for mesolite, the alteration mineral assemblage predicted from the model is nearly identical to that in chondrules of the CV carbonaceous chondrites. Saponite has been widely recognized in chondrules of CV chondrites. It occurs as replacing enstatite and mesostasis. Serpentine also occurs as intergrowth with saponite. It is widely known that, in CV chondrites, diopside has showed more strongly resistance to alteration compared with any other minerals and has been widely occurred as relict mineral of alteration. These results suggest that chondrules of CV chondrites have been probably affected by minor degree of aqueous alteration similar to the system in the model, including only enstatite and mesostasis phases.

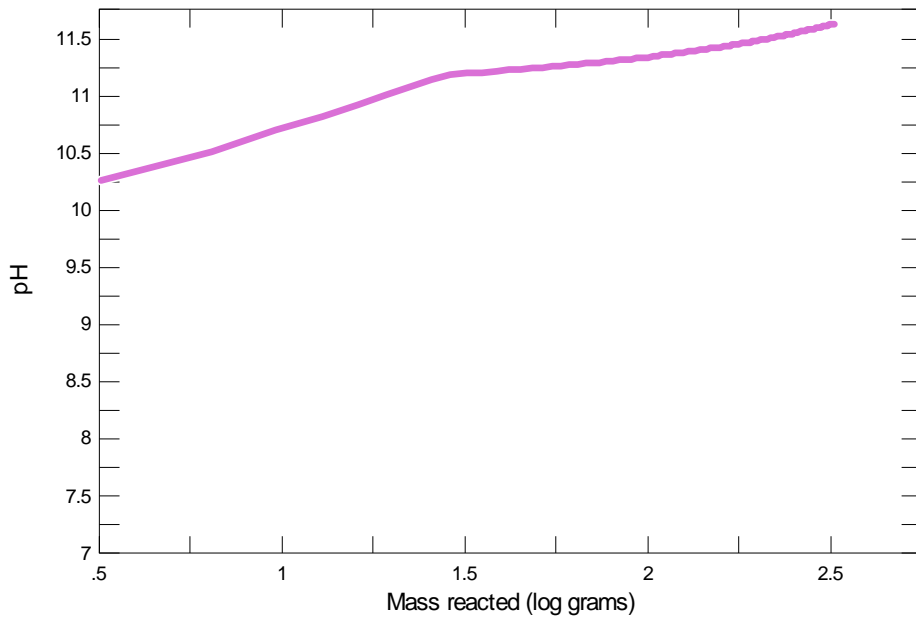


12/25/01 Fri Nov 01 2002

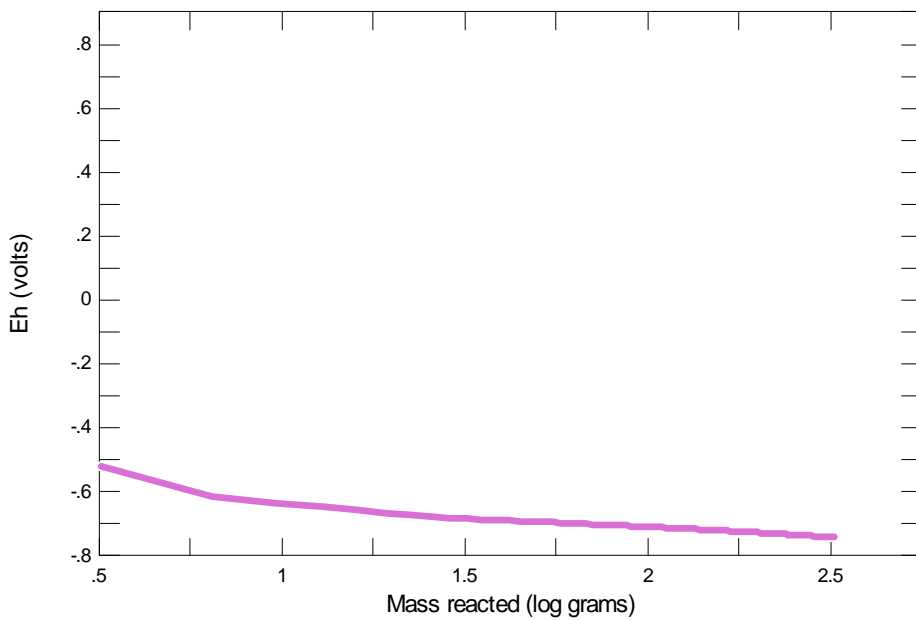


12/25/01 Fri Nov 01 2002

Figure 7.1: Calculation results from *Model 1* (POP), showing alteration mineral assemblage (upper) and dissolved ions in aqueous solution (lower).

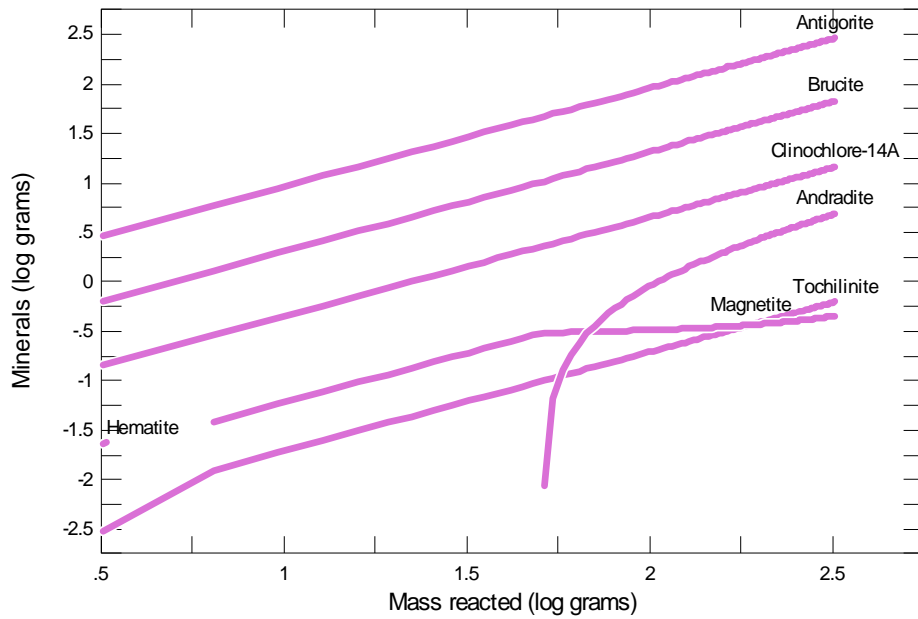


88 12:51 PM Fri Nov 01 2002

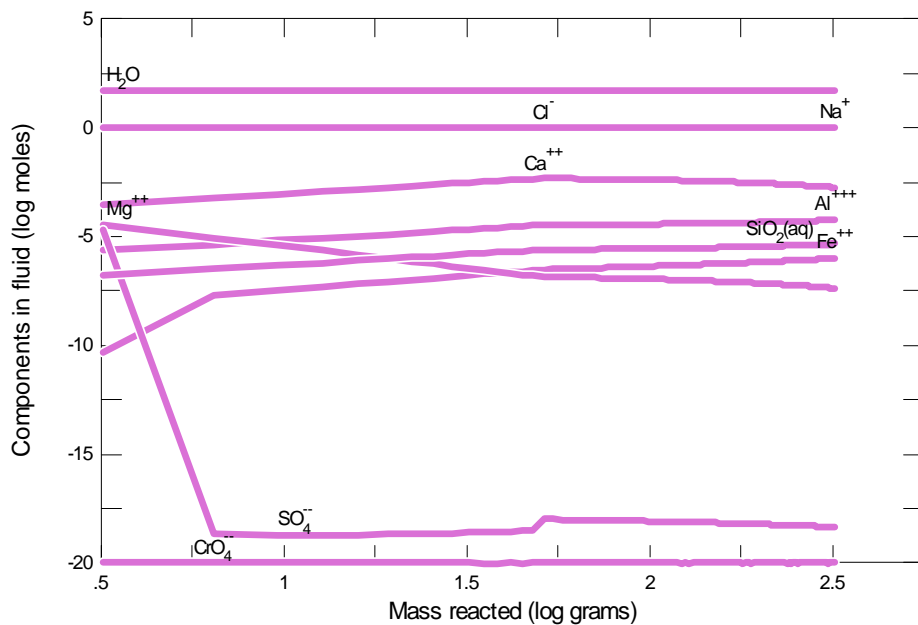


88 12:51 PM Fri Nov 01 2002

Figure 7.1: *Continued.* Calculation results from *Model 1* (POP), showing pH values (upper) and Eh values (lower) in aqueous solution.

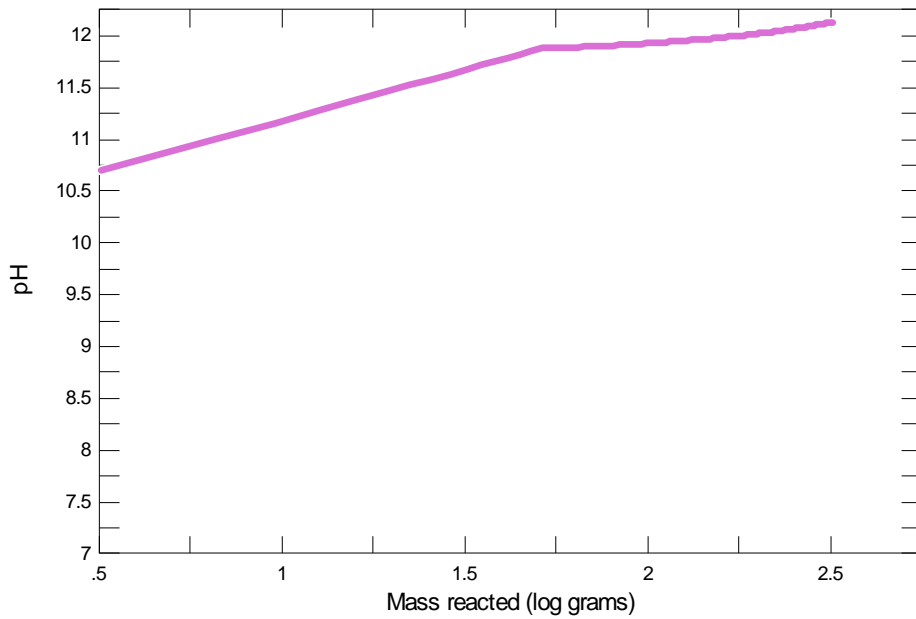


88 12:51N Fri Nov 01 2002

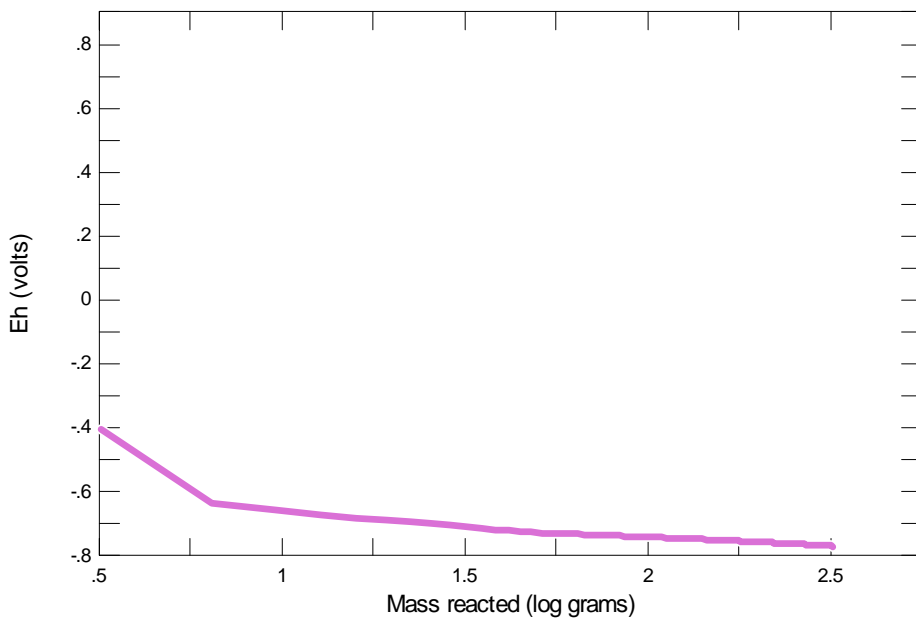


88 12:51N Fri Nov 01 2002

Figure 7.2: Calculation results from *Model 1* (PO), showing alteration mineral assemblage (upper) and dissolved ions in aqueous solution (lower).

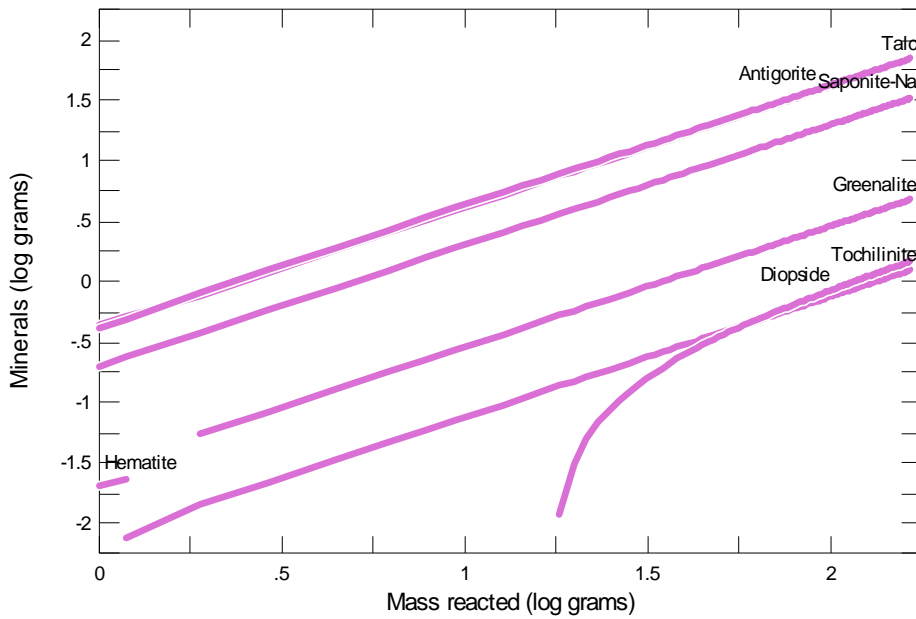


88 12:51 PM Fri Nov 01 2002



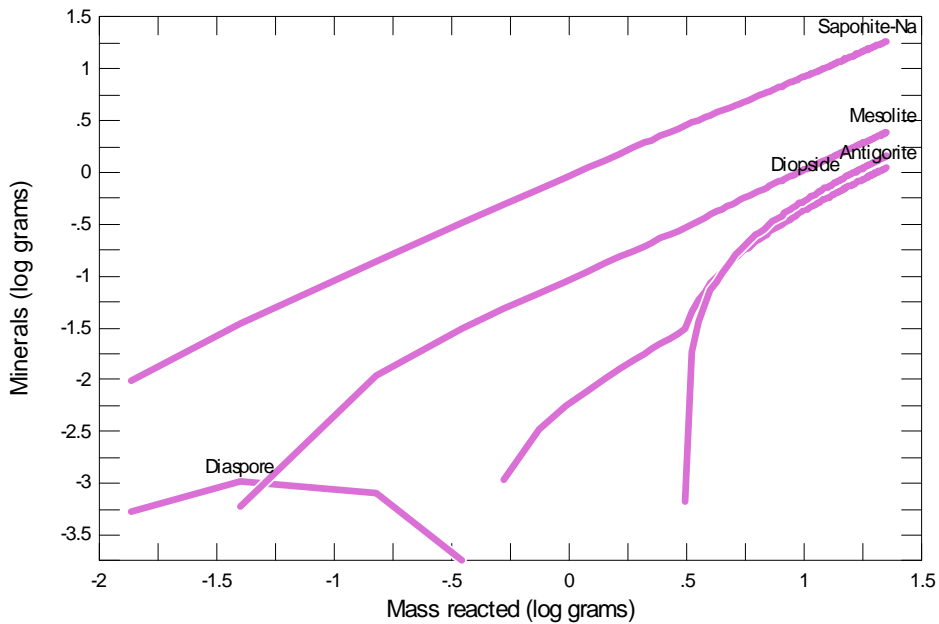
88 12:51 PM Fri Nov 01 2002

Figure 7.2: *Continued.* Calculation results from *Model 1* (PO), showing pH values (upper) and Eh values (lower) in aqueous solution.



12:51 PM Fri Nov 01 2002

Figure 7.3: Calculation result from *Model 2*, showing alteration mineral assemblage.



12:51 PM Fri Nov 01 2002

Figure 7.4: Calculation result from *Model 3*, showing alteration mineral assemblage.

Conclusions for Part II

I assumed three models for aqueous alteration of chondrules, including equilibrated and unequilibrated alteration. Using the REACT computer code, I predicted alteration mineral assemblages of chondrules in heavily altered CM chondrites, weakly to moderately altered CM chondrites and altered CV chondrites, suggesting that phyllosilicate mineralogy vary from saponite-domain to serpentine-domain with alteration progress. The results revealed that the variation of precursor mineral assemblage involved in aqueous alteration would cause the variation of alteration mineral assemblage. At the earliest stage of aqueous alteration, constituent minerals having low resistance to alteration (*e.g.*, mesostasis phases, enstatite, Fe-Ni metal and sulfide) would be more strongly modified compared with any other minerals. Therefore, in order to clarify detail about mechanism of aqueous alteration of chondrules, we need to understand how these minerals have been affected by aqueous fluid. And we must reveal kinetics of alteration of each constitute mineral (*e.g.*, enstatite) in chondrules (see Part I).

References for Part II

Bethke C. M. (1996) *Geochemical Reaction Modeling: Concepts and Applications*. Oxford University Press, New York, New York, USA. 397 pp.

Bourcier W. and Zolensky M. (1991) Aqueous alteration on the parent bodies of carbonaceous chondrites: Computer simulations of late-stage oxidation (abstract). *54th Annual Meeting of the Meteoritical Society*, 30.

Bourcier W. and Zolensky M. (1992) Computer modeling of aqueous alteration on carbonaceous chondrite parent bodies. *Lunar Planet. Sci.* **23**, 143-144.

Brearley A. J. and Jones R. H. (1998) Chondritic meteorites. In *Planetary Materials* (ed. J. J. Papike), Rev. Mineral., **36**. Mineralogical Society of America, Washington, USA.

Browning L. and Bourcier W. (1996) Tochilinite: A sensitive indicator of alteration conditions on the CM asteroidal parent body (abstract). *Lunar Planet. Sci.* **27**, 171-172.

Browning L. and Bourcier W. (1998) Constraints on the anhydrous precursor mineralogy of fine-grained materials in carbonaceous chondrites. *Meteorit. Planet. Sci.* **33**, 1213-1220.

Grimm R. E. and McSween H. Y. Jr. (1989) Water and the thermal evolution of carbonaceous chondrite parent bodies. *Icarus* **82**, 244-280.

Grossman J. N., Rubin A. E., Nagahara H., and King E. A. (1988) Properties of chondrules. In *Meteorites and the Early Solar System* (eds. J.F. Kerridge and M.S. Matthews), pp. 619-659. Univ. Arizona, Tucson, Arizona.

Hanowski N. P. and Brearley A. J. (2001) Aqueous alteration of chondrules in the CM carbonaceous chondrite, Allan Hills 81002: Implications for parent body alteration. *Geochim. Cosmochim. Acta* **65**, 495-518.

- Johnson J. W., Oelkers E. H., and Helgeson H. C. (1992) SUPCRT92: A software package for calculating the standard molal thermodynamic properties of minerals, gases, aqueous species, and reactions from 1 to 5000 bars and 0 to 1000°C. *Compt. Geosci.* **18**, 899-947.
- Jones R. H. (1994) Petrology of FeO-poor, porphyritic pyroxene chondrules in the Semarkona chondrite. *Geochim. Cosmochim. Acta* **58**, 5325-5340.
- McSween H. Y. (1979) Alteration in CM carbonaceous chondrites inferred from modal and chemical variations in matrix. *Geochim. Cosmochim. Acta* **43**, 1761-1770.
- Rosenberg N. D., Browning L., and Bourcier W. L. (2001a) Aqueous alteration of CM carbonaceous chondrites (abstract). *Lunar Planet. Sci.* **XXXII** #1406.
- Rosenberg N. D., Browning L., and Bourcier W. L. (2001b) Modeling aqueous alteration of CM carbonaceous chondrites. *Meteorit. Planet. Sci.* **36**, 239-244.
- Rubin A. E. and Wasson J. T. (1986) Chondrules in the Murray CM2 meteorite and compositional differences between CM-CO and ordinary chondrite chondrules. *Geochim. Cosmochim. Acta* **50**, 307-315.
- Sato K, Miyamoto M., and Mikouchi T. (2002) Hydrothermal experiments on several chondrites at low temperatures: pH change of solution (abstract). **65th Annual Meteoritical Society Meeting** #5133.
- Tomeoka and Buseck (1985) Indicators of aqueous alteration in CM carbonaceous chondrites: Microtextures of a layered mineral containing Fe, S, O and Ni. *Geochim. Cosmochim. Acta* **49**, 2149-2163.
- Wallendahl A. and Treiman A. H. (1999) Geochemical models of low-temperature alteration of Martian rocks (abstract). *Lunar Planet. Sci.* **XXX** #1268.
- Wolery T. J. (1992) *EQ3/6, A software Package for Geochemical Modeling of Aqueous Systems: Package Overview and Installation Guide*. UCRL-MA-110662. Lawrence Livermore National Laboratory, Livermore, California, USA. 66 pp.

Zolensky M., Bourcier W. and Gooding J. L. (1988) Computer modeling of the mineralogy of the Martian surface, as modified by aqueous alteration. In *Lunar and Planetary Inst., Workshop on Mars Sample Return Science* pp. 188-189

Zolensky M., Bourcier W., and Gooding J. L. (1989) Aqueous alteration on the hydrous asteroids: Results of EQ3/6 computer simulations. *Icarus* **78**, 411-425.

Zolensky M. E., Mittlefehldt D. W., Lipshutz M. E., Wang M.-S., Clayton R. N., Mayeda T. K., Grady M. M., Pillinger C., and Barber D. (1997) CM chondrites exhibit the complete petrologic rang from type 2 to 1. *Geochim. Cosmochim. Acta* **61**, 5099-5115.

Chapter 8

Concluding Remarks of This Thesis

In part I, I reported the results of hydrothermal experiments of enstatite. Although hydrous phyllosilicates have been readily formed by hydrothermally alteration of enstatite in the present experiments, the assemblages of produced phyllosilicates were affected by pH and compositions of aqueous solution. And there is a difference in resistance to alteration between different crystal polymorphs of enstatite. From these results, I suggested that primary mineral assemblage involved in aqueous alteration is a main factor controlling the alteration mineral assemblage of enstatite. In part II, I also reported that alteration mineral assemblage in chondrules depends strongly on precursor mineral assemblage involved in aqueous system from results of the computer modeling.

Primary, precursor mineral assemblages involved in aqueous alteration probably have been associated with water/rock ratio together with initial pH value of aqueous fluid. So, I concluded that water/rock ratio is one of the most indicative quantitative parameters controlling the aqueous alteration process of chondrules. In altered chondrules of CV chondrites that contain relatively small amounts of smectite-dominated phyllosilicates, water/rock ratio must have been relatively low. In chondrules of most CM chondrites that contain abundant amounts of serpentine-dominated phyllosilicates, water/rock ratio must have been high. The difference in water/rock ratio during aqueous alteration between these chondrite clans is quite uncertain at present. It may be that the difference in ice/anhydrous rock ratio between the carbonaceous chondrite parent bodies, presumed that originally consisted of a heterogeneous mixture of ice and anhydrous rock (Grimm and McSween, 1989).

Acknowledgement

I would like to acknowledge Professor Kazushige Tomeoka for introducing the planetary material science to me and discussing with me about subject of research. I learned so much about the science from him and I am honored to study as a member of his students. I would like to acknowledge Professor Hiroaki Sato and Professor Tadashi Mukai for obtaining valuable comments on this thesis. I would like to acknowledge Professor Kazuaki Iishi, Professor Akira Tsuchiyama, Dr. Takaaki Noguchi, Dr. Shogo Tachibana, Mr. Shinji Inoue, for the preparation of orthoenstatite crystals. I would like to acknowledge Professors Takabumi Sakamoto, Katsutoshi Tomita, Motoharu Kawano, Tsutomu Sato, for valuable comments about clay minerals. I would like to acknowledge Professor Takashi Murakami, Dr. Keisuke Fukushi, for valuable comments about computer modeling. I gratefully thank Dr. Tomoko Kojima and Dr. Naotaka Tomioka for valuable discussion and technical support. I thank all of my colleagues in the Planetary Material Science Laboratory of Kobe University for their useful and enjoyable discussions. Finally, I am grateful to my family for their infinite support. Thank you so much.

Ichiro Ohnishi